SIAM J. APPL. MATH.
Vol. 58, No. 6, pp. 1969–1995, December 1998
© 1998 Society for Industrial and Applied Mathematics
016

ASYMPTOTIC TRANSMISSION OF SOLITONS THROUGH RANDOM MEDIA*

JOSSELIN GARNIER†

Abstract. This paper contains a study of the transmission of a soliton through a slab of nonlinear and random media. A random nonlinear Schrödinger equation is considered, where the randomness holds in the potential and the nonlinear coefficient. Using the inverse scattering transform, we exhibit several asymptotic behaviors corresponding to the limit when the amplitudes of the random fluctuations go to zero and the size of the slab goes to infinity. The mass of the transmitted soliton may tend to zero exponentially (as a function of the size of the slab) or following a power law, or else the soliton may keep its mass, while its velocity decreases at a logarithmic rate or even more slowly. Numerical simulations are in good agreement with the theoretical results.

Key words. nonlinear Schrödinger equation, inverse scattering transform, solitons, random media, diffusion-approximation

AMS subject classifications. 60F05, 35Q55

PII. S0036139997318573

1. Introduction.

This paper is concerned with the competition between randomness and nonlinearity for wave propagation phenomena in the one-dimensional case [4, 14]. As is well known, in one-dimensional linear media with random inhomogeneities strong localization occurs [3], which means in particular that the transmitted intensity decays exponentially as a function of the size of the medium [15]. On the other hand, in nonlinear media without inhomogeneities, localized wavepackets called solitons can be generated, which propagate with constant velocities over very large distances [17]. We study the transmission of a soliton through a slab of nonlinear and random media. We consider the one-dimensional Schrödinger equation with cubic nonlinearity, and we assume that inhomogeneities affect the potential and the nonlinear coefficient. Kivshar et al. [12] obtained results in the case of a random medium consisting of pure point impurities with very low density which affects only the potential. In such conditions the authors showed that there is a threshold below which the pulses decay quickly. This fact was experimentally observed in [10]. Knapp [13] considered the case of a potential piecewise constant over intervals larger than the width of the soliton. He developed an approximate theory based on an equivalent particle method and compared it to direct numerical simulations. We shall consider more general types of perturbations and proceed under a different asymptotic framework. We actually consider the effects of small random perturbations and aim to exhibit the possible asymptotic behaviors when the amplitudes of the random fluctuations go to zero and the size of the slab goes to infinity.

An application may be communication in optical fibers [9], which consists of sending binary messages at a very high rate. Indeed, a sequence of "0" and "1" can be coded as a train of short pulses, where a "1" is represented by a pulse and a "0" by the absence of a pulse in the corresponding arrival time slot of the train. The success of this method is based on the fact that modern technology has succeeded

*Received by the editors March 21, 1997; accepted for publication (in revised form) January 16, 1998; published electronically August 20, 1998.
http://www.siam.org/journals/siap/58-6/31857.html
†Centre de Mathématiques Appliquées, Ecole Polytechnique, 91128 Palaiseau Cedex, France, (garnier@cmapx.polytechnique.fr).

in producing purified glass fiber with a very low level of attenuation. Unfortunately another phenomenon appears to be a limitation to the race towards higher and higher transmission rates. Indeed, dispersion makes wavepackets spread out. This effect is, moreover, increased for high communication rates, since it is proportional to the square of the time width of a pulse. However, nonlinear effects such as self-focusing compete with dispersion. The nonlinear Schrödinger equation, which describes this competition to a good approximation, has a special solution, the so-called soliton, for which the nonlinear effects exactly counterbalance dispersion. It is therefore a good candidate for the information bit in the next generation of optical fibers [8]. In order to confirm this hope, it is relevant to study the behavior of a soliton when it propagates through weakly perturbed media over very large distances.

The paper is organized as follows. In section 2 we review the main features of the well-known inverse scattering transform that will be used throughout the paper. In section 3 we present the problem of the propagation of a soliton through a random slab. The next two sections are devoted to the analysis of the problem at hand under the so-called adiabatic approximation. In section 6 we show the convergence of the characteristics of the transmitted soliton, whose asymptotic behaviors are studied in section 7. In section 8 we check a posteriori the adiabatic approximation for consistency. Finally some numerical simulations are presented in section 9. There is also an additional section which contains technical estimates and mixing lemmas.

2. The homogeneous nonlinear Schrödinger equation.

For more detail about the following statements and their proofs we refer to [1, 17, 18].

2.1. An introduction to the inverse scattering transform.

The scattering transform aims at studying the solutions of nonlinear partial differential equations of the type $u_t = F(u)$ with rapidly decaying initial conditions. It can be applied in the case where the evolution equation is equivalent to an equality between linear operators:

$$\frac{\partial L(u)}{\partial t} + [L, A] = 0. \tag{1}$$

It is based on the fact that $u(t, .)$ can be characterized by some spectral data of the operator $L(u(t, .))$. The homogeneous nonlinear Schrödinger equation (NLS)

$$iu_t + u_{xx} + 2|u|^2 u = 0 \tag{2}$$

can be expressed in the form (1) if we set

$$L(u) = iP\frac{\partial}{\partial x} + Q(u), \text{ with } P = \begin{pmatrix} 1 & 0 \\ 0 & -1 \end{pmatrix} \text{ and } Q(u) = \begin{pmatrix} 0 & u^* \\ -u & 0 \end{pmatrix}.$$

The operator A is of the type $-2iP\frac{\partial^2}{\partial x^2} + C(u)$, with $C(u) \to 0$ when $u \to 0$, $u_x \to 0$. The domain of $L(u)$ is the space $\mathbb{H}^1(\mathbb{R})$,

$$\mathbb{H}^1(\mathbb{R}) = \left\{ \psi \text{ such that } \psi \in \mathbb{L}^2(\mathbb{R}), \psi_x \in \mathbb{L}^2(\mathbb{R}) \right\},$$

which is a dense subset of the Hilbert space $\mathbb{L}^2(\mathbb{R})$:

$$\mathbb{L}^2(\mathbb{R}) = \left\{ \psi = \psi_1 \mathbf{e_1} + \psi_2 \mathbf{e_2}, \psi_j \in L^2(\mathbb{R}) \right\}, \quad \mathbf{e_1} = \begin{pmatrix} 1 \\ 0 \end{pmatrix}, \quad \mathbf{e_2} = \begin{pmatrix} 0 \\ 1 \end{pmatrix}$$

equipped with the scalar product

$$\langle \psi, \phi \rangle = \int_{-\infty}^{+\infty} dx \psi_1^* \phi_1(x) + \psi_2^* \phi_2(x).$$

Operator $L(0)$. $L(0)$ is self-adjoint. The real axis constitutes its essential spectrum. The eigenspace associated with the eigenvalue $\lambda \in \mathbb{R}$ has dimension 2 and admits the couple $\left(\mathbf{e_1}e^{-i\lambda x}, \mathbf{e_2}e^{i\lambda x}\right)$ as a base. Besides, the point spectrum of $L(0)$ is empty, because the nontrivial solutions of $v_x = i\lambda v$ are not in $L^2(\mathbb{R})$.

Essential spectrum of the operator $L(u(t = t_0, .))$. Let us consider the spectral problem associated with the operator $L(u) = L(0) + Q(u)$:

$$L(u(t,x))\psi(t,x) = \lambda(t)\psi(t,x), \quad \psi = \psi_1\mathbf{e_1} + \psi_2\mathbf{e_2}. \tag{3}$$

If $u(t = t_0, .) \in L^1(\mathbb{R})$, then $Q(u)$ is $L(0)$-compact. As a consequence of the Weyl theorem, the essential spectrum of $L(u)$ is equal to the real axis. Equation (3) actually admits two linearly independent solutions when λ is real. The so-called Jost functions f and g are the eigenfunctions of $L(u)$ which are associated with the real eigenvalue λ and which satisfy the following boundary conditions:

$$f(x,\lambda) \overset{x\to+\infty}{\longrightarrow} \mathbf{e_2}e^{i\lambda x}, \quad g(x,\lambda) \overset{x\to-\infty}{\longrightarrow} \mathbf{e_1}e^{-i\lambda x}.$$

If we denote by $\bar{\psi}$ the vector $(\psi_2^*, -\psi_1^*)$ associated with a vector ψ solution of (3), then $\bar{\psi}$ is a solution of $L\bar{\psi} = \lambda^*\bar{\psi}$. In the case of a real eigenvalue, ψ and $\bar{\psi}$ are linearly independent and form a base of the space of the solutions of (3). It can then be proved that the Jost functions are related by

$$g(x,\lambda) = a(\lambda)\bar{f}(x,\lambda) + b(\lambda)f(x,\lambda), \quad f(x,\lambda) = -a(\lambda)\bar{g}(x,\lambda) + b^*(\lambda)g(x,\lambda). \tag{4}$$

Injecting the second equality into the first one, we also exhibit the following conservation relation:

$$|a(\lambda)|^2 + |b(\lambda)|^2 = 1. \tag{5}$$

Using (3) we get two more conservation relations which concern the norms of the Jost functions f and g:

$$|f_1(x,\lambda)|^2 + |f_2(x,\lambda)|^2 = 1, \qquad |g_1(x,\lambda)|^2 + |g_2(x,\lambda)|^2 = 1.$$

Multiplying the first equality of (4) by the vector $\bar{f}^*$, we get an explicit representation of the coefficient a as the Wronskian of f and g:

$$a(\lambda) = g_1(x,\lambda)f_2(x,\lambda) - g_2(x,\lambda)f_1(x,\lambda). \tag{6}$$

We are able to provide a more explicit representation of the Jost functions f and g. Denoting $\tilde{f}_1(x,\lambda) = e^{i\lambda x}f_1(x,\lambda)$ and $\tilde{f}_2(x,\lambda) = e^{-i\lambda x}f_2(x,\lambda)$, we can find from (3) that $\tilde{f}$ satisfies a system of integral equations. Besides, $\tilde{f}_1$ can be eliminated from this system by substitution, so that we get a closed equation for $\tilde{f}_2$, whose solution is

$$\tilde{f}_2(x,\lambda) = 1 + \int_x^\infty dyM(y,x,\lambda)\left(1 + \int_y^\infty dzM(z,x,\lambda)\,(...)\right),$$

where $M(y,x,\lambda) = -u^*(y)\int_x^y dzu(z)e^{2i\lambda(y-z)}$. This expression holds true when $u \in L^1$, because the associated sequence absolutely converges. The function $\tilde{f}_1$ also admits a similar representation. Let us examine carefully the properties of $\tilde{f}$. If $y \mapsto |y|^n|u(y)| \in L^1$, then $\tilde{f}_1$ and $\tilde{f}_2$ are of class $\mathcal{C}^n$ over the real axis. Besides, if $u \in L^1$, then $\tilde{f}_1$ and $\tilde{f}_2$ can be analytically continued in the upper complex half-plane $\mathrm{Im}(\lambda) \geq 0$, where they have no singularity. Indeed, in view of the definition of M one can see that the exponential term has a norm equal to $e^{-2\mathrm{Im}\lambda(y-z)}$ (remember that we integrate over the domain $y - z > 0$) which decays faster than any polynomial term brought by the λ-derivatives.

Point spectrum of the operator $L(u(t=t_0,.))$. From (6) we can define an analytic continuation of $a(\lambda)$ over the upper complex half-plane. A noticeable feature then appears. If λ_r is a zero of $a(\lambda)$, then f and g are linearly dependent, so there exists a coefficient ρ_r such that $g(x,\lambda_r)=\rho_r f(x,\lambda_r)$. The corresponding eigenfunction is bounded and decays exponentially as $x\to+\infty$ (because $|f|\sim e^{-\mathrm{Im}\lambda_r x}$) and as $x\to-\infty$ (because $|g|\sim e^{+\mathrm{Im}\lambda_r x}$). Thus λ_r is an element of the point spectrum of $L(u)$. Moreover we can compute from (3) and (6) the λ-derivative of a at $\lambda=\lambda_r$:

$$a'(\lambda_r) = -2i\rho_r \int_{-\infty}^{+\infty} dx f_1 f_2(x,\lambda_r). \tag{7}$$

It can be proved that the set $(a(\lambda),b(\lambda),\lambda_r,\rho_r,a'(\lambda_r))$ characterizes the Jost functions f and g and the solution u. The inverse transform is essentially based on the resolution of the linear integrodifferential Gelfand–Levitan–Marchenko equation, whose entries are constituted by the set $(a,b,\lambda_r,\rho_r,a'(\lambda_r))$:

$$\begin{aligned} &K_1(x,y) = \Phi^*(x+y) - \int_x^\infty K_1(x,y'')\int_x^\infty \Phi^*(y+y')\Phi(y'+y'')dy'dy'',\\ &K_2(x,y) = -\int_x^\infty K_1^*(x,y')\Phi^*(y+y')dy',\\ &\text{where } \Phi(y) = -\sum_r \frac{i\rho_r}{a'(\lambda_r)}e^{i\lambda_r y} + \frac{1}{2\pi}\int_{-\infty}^{+\infty}\frac{b(\lambda)}{a(\lambda)}e^{i\lambda y}d\lambda. \end{aligned} \tag{8}$$

We can get the eigenvector f from the kernel K solution of (8):

$$f(x,\lambda) = \mathbf{e_2}e^{i\lambda x} + \int_x^\infty K(x,y)e^{i\lambda y}dy. \tag{9}$$

We then obtain u by the formula $u(x)=-2iK_1^*(x,x)$. The study of the inverse problem associated with the operator $L(u)$ has not yet been completely achieved. In particular the precise characterization of the spectral data which lead to well-defined potentials u has not yet been completed. However, in the case where the initial condition u_0 is rapidly decaying so that it satisfies $x\mapsto|x|^n|u_0|(x)\in L^1$ for any n, the inverse scattering can be rigorously achieved [1].

The great advantage of the method is that the evolution equations of the scattering data are uncoupled:

$$a(t,\lambda)=a(t_0,\lambda),\quad b(t,\lambda)=b(t_0,\lambda)e^{-4i\lambda^2(t-t_0)},\quad \rho_r(t)=\rho_r(t_0)e^{-4i\lambda_r^2(t-t_0)}.$$

To sum up, the scattering transform involves the following operations:

$$\begin{array}{ccc} u(t_0,x) & \overset{\text{direct scatt.}}{\longrightarrow} & (a,b,\lambda_r,\rho_r,a'(\lambda_r))\,(t_0)\\ \text{NLS}\downarrow & & \downarrow \text{uncoupled evolution equations}\\ u(t,x) & \overset{\text{inverse scatt.}}{\longleftarrow} & (a,b,\lambda_r,\rho_r,a'(\lambda_r))\,(t). \end{array}$$

2.2. Conserved quantities. There exists an infinite number of quantities which are preserved by the homogeneous nonlinear Schrödinger equation (2) as soon as they are well defined [17]. They can be represented as functionals of the solution u or in terms of the scattering data. We shall present here only two of them which are of physical interest.

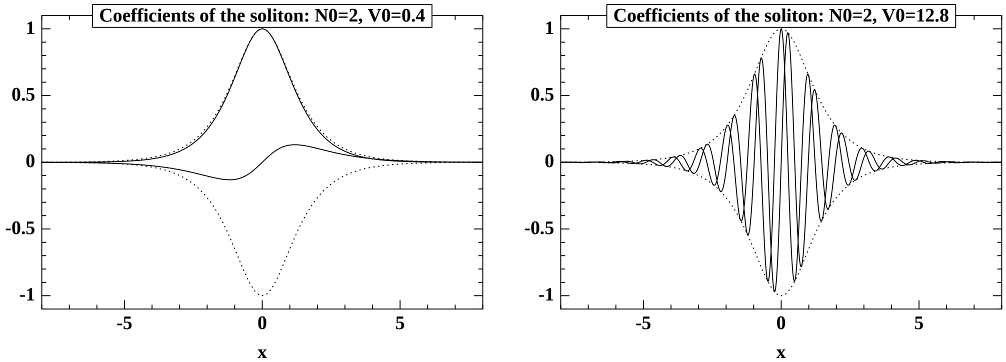

FIG. 1. *Solitons at time $t = 0$. The dashed lines represent the envelopes of the solitons, while the solid lines represent the real and imaginary parts.*

- The mass of the wave $N = \int |u|^2 dx$. Denoting $n(\lambda) = -\pi^{-1} \ln |a(\lambda)|^2$, the mass is also given by

$$N = \sum_r 2i(\lambda_r^* - \lambda_r) + \int n(\lambda) d\lambda. \tag{10}$$

- The Hamiltonian or energy $H = \int |u_x|^2 - |u|^4 dx$, which can also be expressed as

$$H = \sum_r \frac{8i}{3}(\lambda_r^{*3} - {\lambda_r}^3) + 4 \int \lambda^2 n(\lambda) d\lambda. \tag{11}$$

2.3. Soliton. There exists a localized solution (i.e., with finite mass and energy) of the equation (2), which is the so-called soliton solution

$$u_0(t,x) = 2\nu_0 \frac{\exp i\left(2\mu_0(x - 4\mu_0 t) + 4(\nu_0^2 + \mu_0^2)t\right)}{\cosh\left(2\nu_0(x - 4\mu_0 t)\right)}. \tag{12}$$

The mass and the velocity of the soliton are, resp., $N_0 = 4\nu_0$ and $V_0 = 4\mu_0$. The width of the envelope of the soliton is conversely proportional to its mass. The soliton solution (12) is associated with the following scattering data:

$$a_0(\lambda) = \frac{\lambda - (\mu_0 + i\nu_0)}{\lambda - (\mu_0 - i\nu_0)}, \quad b_0(\lambda) = 0. \tag{13}$$

a_0 admits a unique zero in the upper complex half-plane denoted by $\lambda_0 = \mu_0 + i\nu_0$. The coefficient associated with the zero λ_0 is $\rho_0 = i \exp\left(-4i(\mu_0 + i\nu_0)^2 t\right)$. Figure 1 plots two different solitons at time $t = 0$. Both have the same mass, and consequently the same envelope, but they have different velocities. One can notice that, in the case $\nu_0 \gg \mu_0$ (resp., $\nu_0 \ll \mu_0$), the soliton oscillates slowly (resp., quickly) within its envelope.

3. The inhomogeneous problem. We consider from now on a perturbed Schrödinger equation with a nonzero right-hand side:

$$iu_t + u_{xx} + 2|u|^2 u = \varepsilon R(u)(t,x). \tag{14}$$

The small parameter $\varepsilon \in (0,1)$ characterizes the amplitudes of the perturbations. The model of the perturbations is taken to be

$$R(u)(t,x) = V_1(x)u(t,x) + V_2(x)|u|^2(t,x)u(t,x),$$

where V_1 and V_2 are assumed to be bounded functions with compact supports in $[0, L^\varepsilon]$. V_1 characterizes the fluctuations of the linear potential and V_2 the fluctuations of the nonlinear coefficient. We shall assume that the incident wave is a soliton incoming from the left and that V_1 and V_2 are stationary and ergodic random processes. We aim to show that, for a slab of size L/ε^2, the following two statements hold true in the limit $\varepsilon \to 0$. First, the transmitted wave consists of a soliton plus some scattered waves. Second, the soliton dynamics for almost every realization are described by nonrandom evolution equations, where only the Fourier transforms of the autocorrelation functions of the random processes are coming. From the physical point of view this fact was earlier established in [5]. The study of the asymptotic deterministic system will exhibit several possible regimes. Two of them are stable and attractive, the first one being characterized by a logarithmic decay of the velocity for solitons of sufficiently large mass, and the second one by an exponential decay of the mass for solitons of small mass. There are also intermediate regimes, where both the mass and velocity decrease at a polynomial rate. The remainder of the paper is devoted to the statements and proofs of these assertions.

3.1. A priori estimates. First we state a priori estimates of the solution u of Eq. (14).

LEMMA 3.1. 1. *The following quantities (mass and energy) are preserved by the perturbed Schrödinger equation* (14):

$$N_{tot} = \int |u|^2 dx, \quad E_{tot} = \int |u_x|^2 - |u|^4 + \varepsilon V_1(x)|u|^2 + \frac{\varepsilon}{2} V_2(x)|u|^4 dx. \tag{15}$$

2. *The H^1-norm, the L^4-norm, and the L^∞-norm of $u(t,.)$ are uniformly bounded with respect to $t \in \mathbb{R}$ and $\varepsilon \in (0,1)$ by constants which depend only on $\|V_1\|_\infty$ and $\|V_2\|_\infty$.*

Proof. On the one hand, the conservations of the mass and energy are obtained by a usual method and are due to the fact that the functions V_j are real-valued and do not depend on time. On the other hand, substituting the Sobolev inequality $\|v\|_{L^\infty}^2 \le 2\|v\|_{L^2}\|v_x\|_{L^2}$ into the obvious estimate $\|u(t,.)\|_{L^4}^4 \le \|u(t,.)\|_{L^2}^2 \|u(t,.)\|_{L^\infty}^2$, we can deduce from the mass conservation that, for any $\eta > 0$,

$$\|u(t,.)\|_{L^4}^4 \le N_0 \left(\eta^{-1} N_0 + \eta \|u_x(t,.)\|_{L^2}^2 \right). \tag{16}$$

Besides, from the energy conservation,

$$\|u_x(t,.)\|_{L^2}^2 \le E_0 + \left(1 + \frac{\varepsilon}{2}\|V_2\|_\infty\right) \|u(t,.)\|_{L^4}^4 + \varepsilon \|V_1\|_\infty N_0. \tag{17}$$

Substituting (16) into (17) and choosing $\eta = \frac{1}{2} N_0^{-1} \left(1 + \frac{1}{2}\|V_2\|_\infty\right)^{-1}$, we find that the L^2-norm of the derivative u_x is uniformly bounded with respect to $\varepsilon \in (0,1)$ and $t \in \mathbb{R}$. Since the mass is conserved we get the estimate of the H^1-norm. The Sobolev inequality then yields the estimate of the L^∞-norm and (16) provides the estimate of the L^4-norm. $\square$

3.2. Evolutions of the scattering data. We now describe the evolutions of the Jost coefficients a and b during the propagation through a slab contained in the region $[0, L^\varepsilon]$. We assume that the incident wave is a soliton with mass $4\nu_0$ and velocity $4\mu_0$ incoming from the left. The initial scattering data $a(t = -\infty, \lambda)$ and $b(t = -\infty, \lambda)$ are then simply given by (13). They satisfy the following exact equations [11]:

$$(18) \qquad \left\{ \begin{array}{l} \dfrac{\partial a(t,\lambda)}{\partial t} = -\varepsilon \left(a(t,\lambda)\bar{\gamma}(t,\lambda) + b(t,\lambda)\gamma(t,\lambda) \right), \\ \dfrac{\partial b(t,\lambda)}{\partial t} = -4i\lambda^2 b(t,\lambda) + \varepsilon \left(a(t,\lambda)\gamma^*(t,\lambda) + b(t,\lambda)\bar{\gamma}(t,\lambda) \right), \end{array} \right.$$

where the functions γ and $\bar{\gamma}$ are defined by

$$(19) \quad \gamma(t,\lambda) = \int dx R(u)^* f_2^2 + R(u) f_1^2, \quad \bar{\gamma}(t,\lambda) = \int dx R(u) f_1 f_2^* - R(u)^* f_1^* f_2.$$

It thus appears that the perturbations $R(u)$ couple the time evolution equations of the Jost coefficients. We are looking for the final Jost coefficients $a(t = +\infty, \lambda)$ and $b(t = +\infty, \lambda)$ and the associated wave, which will be constructed by the inverse scattering transform.

3.3. Scales and hypotheses. We assume that the amplitudes of the fluctuations are of order $\varepsilon \ll 1$, and that the perturbed slab, i.e., the support of the functions V_j, is contained in the interval $[0, L/\varepsilon^2]$. The functions V_j are assumed to be zero-mean, independent, stationary, and ergodic processes under $\mathbb{P}$. The independence hypothesis permits us to omit crossed terms in the calculations, but it can be cut without altering qualitatively the following results. The centering condition can be cut, too. On the one hand, adding a constant potential v_1 involves only a phase modulation of the soliton of the type $e^{iv_1 t}$, which alters neither the mass nor the velocity of the envelope of the soliton. On the other hand, if $\mathbb{E}[V_2] \neq 0$, then it suffices to put this constant coefficient into the nonlinear term of the left-hand side of (14). We shall denote in the following by $\mathcal{F}_s^t$ the σ-algebra generated by $\sigma(V_j(x), s \leq x \leq t, j = 1, 2)$. We shall consider that the processes V_j are not only ergodic, but also ϕ-mixing, i.e., that there exists a function $t \mapsto \phi(t)$ vanishing as $t \to +\infty$ such that

$$\sup_{s>0} \left\{ \mathbb{P}(B/A) - \mathbb{P}(B), A \in \mathcal{F}_0^s, B \in \mathcal{F}_{s+t}^\infty \right\} \leq \phi(t).$$

For technical reasons we shall assume that the function $t \mapsto \phi(t)$ decays at least as t^{-4}. This mixing condition is sufficient to prove all the convergence results that will be needed. However, we believe that it can be weakened and we expect the condition $\phi \in L^{1/2}(\mathbb{R}^+)$ to be optimal.

3.4. The adiabatic approximation. The adiabatic approximation consists of assuming a priori that, while the soliton exists, its evolution and the ones of the emitted waves do not interact. More precisely, we assume that the time evolutions of the Jost coefficients a and b given by (18) depend only on the components of the functions γ and $\bar{\gamma}$ defined by (19) which are associated with the soliton. We are first going to carry out calculations under this approximation, which will provide an expression of the total wave u. A posteriori we shall check in section 8 for consistency that this approximation is actually justified in the asymptotic framework $\varepsilon \to 0$. More precisely we shall show that the components of the functions γ and $\bar{\gamma}$ which correspond to the interplay between the scattered wavepacket and the soliton, or else which originate from the sole effect of the scattered wavepacket, can be considered as negligible terms for the soliton evolution.

3.5. Notations. Let $\delta \in (0,1)$ be real, which is designed to be small with respect to 1, but larger than ε. We define the stopping time T_δ^ε by

$$T_\delta^\varepsilon = \inf\left\{t, \text{ the soliton is destroyed at } t/\varepsilon^2 \text{ or } (\nu(t/\varepsilon^2), \mu(t/\varepsilon^2)) \in D_\delta^c\right\},$$

where D_δ is the open subset of $\mathbb{R}^2$ given by $D_\delta = (\delta, 1/\delta) \times (\delta, 1/\delta)$. We say that the soliton is destroyed when the associated root of the Jost coefficient a no longer exists. If $t \leq T_\delta^\varepsilon/\varepsilon^2$, then we denote by $x_s(t)$ the position of the center of the soliton at time t (defined from the scattering data by (27)) and by $t_s(x)$ the inverse function, i.e., the arrival time of the soliton in x. $\nu(x)$ (resp., $\mu(x)$) is then a shorthand for $\nu(t_s(x))$ (resp., $\mu(t_s(x))$). We finally introduce the stopping point X_δ^ε defined by $X_\delta^\varepsilon/\varepsilon^2 = x_s(T_\delta^\varepsilon/\varepsilon^2)$.

Let $L > 0$. We denote by $\mathcal{C}^0$ the space $\mathcal{C}^0([0,L],\mathbb{R}^2)$ of all the $\mathbb{R}^2$-valued continuous functions equipped with the topology associated to the uniform norm. $Z_l = (\nu_l(x), \mu_l(x))_{x\in[0,L]}$ is the element of $\mathcal{C}^0$ defined as the unique solution of the system of ordinary differential equations:

$$\frac{dZ_l}{dx} = G(Z_l), \quad Z_l(0) = (\nu_0, \mu_0). \tag{20}$$

The function G belongs to $\mathcal{C}^1(\mathbb{R}^2,\mathbb{R}^2)$ and is equal to

$$G(\nu,\mu) = \begin{pmatrix} -\frac{1}{4\pi}\sum_{j=1}^2 \int_{-\infty}^{\infty} |c_j|^2(\nu,\mu,\lambda) d_j(k(\nu,\mu,\lambda))d\lambda \\ -\frac{1}{8\pi}\sum_{j=1}^2 \int_{-\infty}^{\infty} \left(\frac{\lambda^2}{\mu\nu} + \frac{\nu}{\mu} - \frac{\mu}{\nu}\right) |c_j|^2(\nu,\mu,\lambda) d_j(k(\nu,\mu,\lambda))d\lambda \end{pmatrix}, \tag{21}$$

where the functions c_j are defined by

$$\left\{\begin{aligned} c_1(\nu,\mu,\lambda) &= \frac{\pi}{2^4\mu^3}\frac{(\lambda-\mu+i\nu)^2}{\cosh\left(\pi(\mu^2-\nu^2-\lambda^2)/(4\mu\nu)\right)} \\ c_2(\nu,\mu,\lambda) &= \frac{\pi}{3\times 2^6\mu^5}\frac{(\lambda-\mu+i\nu)^2\left((\lambda+\mu)^2+\nu^2\right)\left(\nu^2+17\mu^2-6\lambda\mu+\lambda^2\right)}{\cosh\left(\pi(\mu^2-\nu^2-\lambda^2)/(4\mu\nu)\right)}, \end{aligned}\right. \tag{22}$$

and the coefficients d_j and k by

$$d_j(k) = 2\int_0^\infty \mathbb{E}[V_j(0)V_j(t)]\cos(kt)dt, \quad k(\nu,\mu,\lambda) = \frac{(\lambda-\mu)^2+\nu^2}{\mu}. \tag{23}$$

In the following we shall denote by K_δ and C_δ constants which depend only on δ, but whose values may change from line to line.

4. Jost coefficients under the adiabatic approximation. We shall first give an accurate and useful expression of the scattering data in Proposition 4.1 then give an estimate of connected integrals.

PROPOSITION 4.1. *Under the adiabatic approximation, if* $T \leq T_\delta^\varepsilon$, *then the scattering data* $\bar{b}/a(t,\lambda) = b/a(t,\lambda)e^{4i\lambda^2 t}$ *at time* T/ε^2 *are given by*

$$\begin{aligned} &\frac{\bar{b}}{a}\left(\frac{T}{\varepsilon^2},\lambda\right) = -i\varepsilon\sum_{j=1}^2\int_0^{x_s(T/\varepsilon^2)} c_j(\lambda,\mu(x),\nu(x))e^{i\psi_s(x,\lambda)}V_j(x)dx, \\ &\psi_s(x,\lambda) = \phi_s(x) - 2\lambda x + 4\lambda^2 t_s(x), \end{aligned} \tag{24}$$

where $x_s(t)$ *is the position of the center of the soliton at time* t *defined by* (27), $t_s(x)$ *is the arrival time of the soliton at point* x, $\phi_s(x)$ *is the phase defined by* (27) *of the soliton when its center is at* x, *and the coefficients* c_j *are given by* (22).

Proof. Under the adiabatic approximation, (18) becomes a closed stochastic system, so that the equation which governs the evolution of the coefficient $\bar{b}/a$ is, for any $t \leq T_\delta^\varepsilon/\varepsilon^2$ [11],

$$\frac{\partial \bar{b}/a}{\partial t} = -i\varepsilon \frac{A(\nu(t),\mu(t),x_s(t),\lambda)e^{i(\phi_s(t)-2\lambda x_s(t)+4\lambda^2 t)}}{(\lambda-\mu(t)-i\nu(t))^2},$$

where A is given after the change of variables $x \mapsto z = 2\nu(t)(x-x_s(t))$ in the integrals (19) by

$$A(\nu,\mu,x_s,\lambda) = \sum_{j=1}^{2}\int_{-\infty}^{+\infty} dz e^{i(\mu-\lambda)z/\nu} B_j(\nu,\mu,z,\lambda)V_j\left(\frac{z}{2\nu}+x_s\right),$$
$$B_j(\nu,\mu,z,\lambda) = \left(\frac{\nu^2}{\cosh^2 z} + (\lambda-\mu-i\nu\tanh z)^2\right)\frac{(2\nu)^{2j-2}}{\cosh^{2j-1} z}.$$

We restrict ourselves to times $T \leq T_\delta^\varepsilon$, so that the L^∞-norm of the Jacobian of the change of variables $t \mapsto x = x_s(t)$ is brought under control. While $t \leq T_\delta^\varepsilon/\varepsilon^2$, this function is invertible, with inverse $t_s(x)$, the arrival time at point x of the soliton. The x-derivatives of μ, ν, ϕ_s, and t_s can be estimated up to terms of order ε^2 by [11]:

$$(25)\quad \left|\frac{d\mu}{dx}\right| \leq K_\delta\varepsilon^2, \quad \left|\frac{d\nu}{dx}\right| \leq K_\delta\varepsilon^2, \quad \left|\frac{d\phi_s}{dx} - \frac{\mu^2+\nu^2}{\mu}\right| \leq K_\delta\varepsilon^2, \quad \left|\frac{dt_s}{dx} - \frac{1}{4\mu}\right| \leq K_\delta\varepsilon^2.$$

After some standard transformations which are shown explicitly in [6], where we use tabulated formulae [7, Formula 3.985], we establish the representation (24). ∎

We denote by Γ_L^ε the finite subset of the interval $[0, L/\varepsilon^2]$ defined by

$$\Gamma_L^\varepsilon = \left\{\frac{kL}{\varepsilon^2[|\ln\varepsilon|^{1/2}]}, k = 1,\dots,[|\ln\varepsilon|^{1/2}]\right\}.$$

In the following $a(x,\lambda)$ (resp., $b(x,\lambda)$) is a shorthand for the quantity $a(t_s(x),\lambda)$ (resp., $b(t_s(x),\lambda)$. While $x \leq X_\delta^\varepsilon/\varepsilon^2$, there is no ambiguity in this definition since $x \mapsto t_s(x)$ is one-to-one.

LEMMA 4.2. *If* P *is a function of class* $\mathcal{C}^2$ *with polynomial growth, then there exists a constant* K_δ *such that, for any* $x_s, y \in [0, L/\varepsilon^2]$ *and* $\varepsilon \in (0,1)$,

$$\mathbb{E}\left[|Q^\varepsilon(x_s)|^2\,\mathbb{I}_{x_s\leq X_\delta^\varepsilon/\varepsilon^2}\right] \leq K_\delta\varepsilon^2|\ln\varepsilon|^2, \text{ where } Q^\varepsilon(x_s) = i\int \frac{b}{a}(x_s,\lambda)P(\lambda)e^{2i\lambda y}d\lambda.$$

We can, moreover, insert the supremum $\sup_{x_s\in\Gamma_L^\varepsilon}$ *inside the expectation without changing the estimate.*

We shall state and apply many technical estimates throughout the paper. Most of them are very similar, so we shall give the detailed proof of Lemma 4.2 in subsection 10.1, while we shall only sketch out the proofs of the following lemmas and propositions.

5. Transmitted wave under the adiabatic approximation. In this section we aim to show that the total wave is constituted on the one hand by a soliton, whose mass and velocity will be studied, and on the other hand by a scattered wavepacket whose characteristics will be discussed.

PROPOSITION 5.1. *If $t \leq T^\varepsilon_\delta$, neglecting the terms of higher order, the total wave is given by the sum $u(t/\varepsilon^2, x) = u_S(t/\varepsilon^2, x) + u_L(t/\varepsilon^2, x)$, where u_S is a soliton of mass $4\nu(t/\varepsilon^2)$ and velocity $4\mu(t/\varepsilon^2)$:*

$$u_S\left(\frac{t}{\varepsilon^2}, x\right) = -2i\nu \frac{\exp i\left(2\mu(x-x_s)+\phi_s\right)}{\cosh\left(2\nu(x-x_s)\right)}. \tag{26}$$

x_s and ϕ_s are, resp., the position and the phase of the soliton at time t/ε^2:

$$x_s = \frac{1}{2\nu}\ln\left(\frac{1}{2\nu}\left|\frac{\rho_r(t/\varepsilon^2)}{a'(t/\varepsilon^2,\lambda_s)}\right|\right), \quad \phi_s = \arg\left(-i\frac{\rho_r(t/\varepsilon^2)}{a'(t/\varepsilon^2,\lambda_s)}\right) + 2\mu x_s. \tag{27}$$

$\lambda_s = \mu(t/\varepsilon^2) + i\nu(t/\varepsilon^2)$ and u_L admits the following expression:

$$\begin{aligned} u_L\left(\frac{t}{\varepsilon^2}, x\right) = & \frac{1}{i\pi}\int_{-\infty}^{\infty} \frac{b}{a}(\lambda)\frac{\left(\lambda-\mu+i\nu\tanh\left(2\nu(x-x_s)\right)\right)^2}{(\lambda-\mu+i\nu)^2} e^{2i\lambda x} d\lambda, \\ & + \frac{\nu^2}{i\pi}\frac{\exp 2i\left(2\mu(x-x_s)+\phi_s\right)}{\cosh^2\left(2\nu(x-x_s)\right)}\int_{-\infty}^{\infty}\frac{b^*}{a^*}(\lambda)\frac{1}{(\lambda-\mu-i\nu)^2}e^{-2i\lambda x}d\lambda. \end{aligned} \tag{28}$$

u_S is the soliton part of the total wave. The first component of u_L represents the scattered wavepacket, with a correction in the neighborhood of the soliton $x \sim x_s(t/\varepsilon^2)$. The second component of u_L represents the interaction between the soliton and the scattered wavepacket, which is only noticeable in the neighborhood of the soliton. From Lemma 4.2, we claim that the amplitude of the scattered wavepacket is at most of order $\varepsilon|\ln\varepsilon|$. This result is not surprising. Indeed, the support of the scattered wavepacket lies in an interval with length of order ε^{-2}. Since its L^2-norm is bounded by the conservation of the total mass, it is natural to find an amplitude of order ε.

Proof. Let us fix $t \leq T^\varepsilon_\delta$. We denote $\bar{b}(t/\varepsilon^2,\lambda) = e^{4i\lambda^2 t/\varepsilon^2} b(t/\varepsilon^2,\lambda)$. The function Φ which appears in (8) is equal to the sum $\Phi_S + \Phi_L$ with

$$\Phi_S\left(\frac{t}{\varepsilon^2}, x\right) = \frac{-i\rho_r}{a'(t/\varepsilon^2,\lambda_s)}e^{i\lambda_s x}, \quad \Phi_L\left(\frac{t}{\varepsilon^2}, x\right) = \frac{1}{2\pi}\int_{-\infty}^{+\infty}\frac{b(t/\varepsilon^2,\lambda)}{a(t/\varepsilon^2,\lambda)}e^{i\lambda x}d\lambda.$$

From Lemma 4.2, the second term $\Phi_L(t/\varepsilon^2, x)$ is of order $\varepsilon|\ln\varepsilon|$. As a consequence Φ_L plays the role of a perturbation of Φ. The kernel K associated with the total wave $u(t/\varepsilon^2, .)$ can be represented as the sum $K_S + K_L$, where

$$K_S(x,y) = \frac{\nu\exp\left((\nu+i\mu)(x-y)\right)}{\cosh\left(2\nu(x-x_s)\right)}\begin{pmatrix} \exp i\left(2\mu(x_s-x)-\phi_s\right) \\ -\exp\left(2\nu(x_s-x)\right)\end{pmatrix}.$$

Neglecting the terms of higher order, K_{L1} is a solution of

$$K_{L1}(x,y) + \int_x^\infty K_{L1}(x,y'')\int_x^\infty \Phi_S^*(y+y')\Phi_S(y'+y'')dy'dy'' = \Psi(x,y),$$

$$\begin{aligned}\Psi(x,y) = \Phi_L^*(x+y) - \int_x^\infty K_{S1}(x,y'')\int_x^\infty & \left(\Phi_S^*(y+y')\Phi_L(y'+y'')\right. \\ & \left. +\Phi_L^*(y+y')\Phi_S(y'+y'')\right)dy'dy''.\end{aligned}$$

The second component can be deduced from

$$K_{L2}(x,y) = -\int_x^\infty K_{S1}^*(x,y')\Phi_L^*(y+y')dy' - \int_x^\infty K_{L1}^*(x,y')\Phi_S^*(y+y')dy'.$$

After some calculations, it can be checked that

$$\begin{aligned} K_{L1}(x,y) = & \frac{1}{2\pi}\int_{-\infty}^\infty d\lambda \frac{b^*}{a^*}(\lambda)e^{-i\lambda(x+y)}\frac{\nu^2+(\mu-\lambda)^2+i\nu(\lambda-\mu+i\nu)\chi_-(x)}{\nu^2+(\mu-\lambda)^2} \\ & +\frac{1}{2\pi}\int_{-\infty}^\infty d\lambda \frac{b^*}{a^*}(\lambda)e^{-2i\lambda x}e^{(i\mu+\nu)(x-y)} \\ & \cdot\frac{i\nu(\nu^2+(\mu-\lambda)^2)\chi_-(x)-\nu^2(\lambda-\mu+i\nu)\chi_-(x)^2}{(\nu^2+(\mu-\lambda)^2)(\lambda-\mu-i\nu)} \\ & +\frac{1}{2\pi}\int_{-\infty}^\infty d\lambda \frac{b}{a}(\lambda)e^{2i\lambda x}\frac{\nu^2 e^{-i\mu(3x+y-4x_s)+\nu(x-y)-2i\phi_s}}{(\lambda-\mu+i\nu)^2\cosh\left(2\nu(x-x_s)\right)^2}, \end{aligned}$$

$$\begin{aligned} K_{L2}(x,y) = & \frac{1}{2\pi}\int_{-\infty}^\infty d\lambda \frac{b^*}{a^*}(\lambda)e^{-i\lambda(x+y)}\frac{i\nu e^{2i\mu(x-x_s)+i\phi_s}}{(\lambda-\mu-i\nu)\cosh\left(2\nu(x-x_s)\right)} \\ & -\frac{1}{2\pi}\int_{-\infty}^\infty d\lambda \frac{b^*}{a^*}(\lambda)e^{-2i\lambda x}\frac{\nu^2 e^{i\mu(3x-y-2x_s)+\nu(2x_s-x-y)+i\phi_s}}{(\lambda-\mu-i\nu)^2\cosh\left(2\nu(x-x_s)\right)^2} \\ & -\frac{1}{2\pi}\int_{-\infty}^\infty d\lambda \frac{b}{a}(\lambda)e^{2i\lambda x}e^{-i\mu(x+y-2x_s)+\nu(2x_s-x-y)-i\phi_s} \\ & \cdot\frac{i\nu(\nu^2+(\mu-\lambda)^2)\chi_+(x)+\nu^2(\lambda-\mu-i\nu)\chi_+\chi_-(x)}{(\nu^2+(\mu-\lambda)^2)\,(\lambda-\mu+i\nu)}, \end{aligned}$$

where $\chi_\pm(x) = 1\pm\tanh\left(2\nu(x-x_s)\right)$. Following the inverse scattering method, we obtain the transmitted wave by the formula $u(t/\varepsilon^2,x) = -2iK_1^*(x,x)$, which establishes the result. ☐

We can now focus on the Jost coefficient a and study the stability of its root in the upper complex half-plane. Obviously this stability conditions the existence of the corresponding soliton.

LEMMA 5.2. *If* $\xi(\varepsilon)\overset{\varepsilon\to 0}{\longrightarrow}+\infty$, *then for any* $x_s\in[0,L/\varepsilon^2]$,

$$\limsup_{\varepsilon\to 0}\mathbb{P}\left(\sup_{\lambda\in B(\delta)}\left|a(x_s,\lambda)-\frac{\lambda-\lambda_s(x_s)}{\lambda-\lambda_s^*(x_s)}\right|\geq\varepsilon|\ln\varepsilon|\xi(\varepsilon),\ x_s\leq\frac{X_\delta^\varepsilon}{\varepsilon^2}\right)=0,$$

where $B(\delta)=\{\lambda\in\mathbb{C},\mathrm{Im}\lambda\geq\delta\}$ *and* $\lambda_s(x_s)=\mu(x_s)+i\nu(x_s)$. *We can, moreover, insert the supremum* $\sup_{x_s\in\Gamma_L^\varepsilon}$ *inside the probability without changing the estimate.*

Proof. Let us first focus on the Jost function f. It can be written as the sum f_S+f_L by (9). The term f_S (resp., f_L) of the expansion is associated with K_S (resp., K_L). If we consider that λ belongs to the upper complex half-plane, $\lambda_1+i\lambda_2$, $\lambda_2>0$, then we can find the complete expressions of f_S and f_L [6]. In particular the expression of f_L is of the same type as that of K_L. By using Lemma 4.2 and discussing the amplitude of the function f_L, we come to the conclusion that f_L can be considered a perturbation of f of the order of $\varepsilon|\ln\varepsilon|$ uniformly with respect to $\lambda_2>\delta$. However, if λ is very close to the real axis, then a resonance appears in (9), so that the uniform estimate in $\varepsilon|\ln\varepsilon|$ is no more valid. We can also do the same for the second Jost function g. Using the relation (6) which expresses the Jost coefficient a as the Wronskian of f and g, we get the result of the lemma. ◻

It thus appears that, in the upper complex half-plane, a remains close to the form $a_s(x_s,\lambda) = (\lambda-\lambda_s(x_s))/(\lambda-\lambda_s^*(x_s))$. However, the coefficient a is much more affected over the real axis. Lemma 5.2 also exhibits that the root of the Jost coefficient a cannot disappear suddenly, in the sense that

$$\limsup_{\varepsilon\to 0}\mathbb{P}\left(X_\delta^\varepsilon < L \text{ and } \forall x_s < X_\delta^\varepsilon/\varepsilon^2, (\nu(x_s),\mu(x_x)) \in D_\delta\right) = 0. \tag{29}$$

Proof of (29). An obvious estimate of a_s shows that $|a_s(x_s,\lambda)| \geq |\ln\varepsilon|^{-1/2}$ for any $|\lambda-\lambda_s| \geq 2\nu|\ln\varepsilon|^{-1/2}$. If $x_s \leq X_\delta^\varepsilon/\varepsilon^2$, then the variation of the coefficient a cannot exceed $K_\delta\varepsilon^2\Delta t$ over the time interval $[t_s(x_s), t_s(x_s)+\Delta t]$. Since Lemma 5.2 provides a control of the L^∞-norm of $a(x_s,.) - a_s(x_s,.)$, this implies that, with a very high probability, $|a(t_s(x_s)+\Delta t,\lambda) - a_s(x_s,\lambda)| < |a_s(x_s,\lambda)|$ for any $|\lambda-\lambda_s| = K_\delta|\ln\varepsilon|^{-1/2}$ and $\Delta t \leq L\varepsilon^{-2}|\ln\varepsilon|^{-1/2}\delta^{-1}$. Applying Rouché's theorem [20, Theorem 10-43], we get that, over the time interval $[t_s(x_s), t_s(x_s) + L\varepsilon^{-2}|\ln\varepsilon|^{-1/2}\delta^{-1})$, there exists a unique zero inside the circular disc with center at λ_s and radius $K_\delta|\ln\varepsilon|^{-1/2}$. In the case where $x_s + L\varepsilon^{-2}|\ln\varepsilon|^{-1/2} \leq \varepsilon^{-2}X_\delta^\varepsilon$, the following inequality is straightforward: $t_s(x_s + L\varepsilon^{-2}|\ln\varepsilon|^{-1/2}) \leq t_s(x_s) + L\varepsilon^{-2}|\ln\varepsilon|^{-1/2}\delta^{-1}$. We can therefore iterate the above argument with respect to $x_s \in \Gamma_L^\varepsilon$ and sum over the $[|\ln\varepsilon|^{1/2}]$ elements. ◻

The interpretation is the following. In the asymptotic framework $\varepsilon \to 0$, the only way we can have $X_\delta^\varepsilon < L$ is for the coefficients of the soliton to escape the domain D_δ. The soliton cannot be destroyed while its velocity and mass are large enough, i.e., larger than δ. Let us now consider the λ-derivative of $a(x_s,.)$ at the point λ_s. From the following lemma we can deduce that the root λ_s is simple.

LEMMA 5.3. *If* $\xi(\varepsilon) \stackrel{\varepsilon\to 0}{\longrightarrow} +\infty$, *then for any* $x_s \in [0, L/\varepsilon^2]$,

$$\limsup_{\varepsilon\to 0}\mathbb{P}\left(\left||a'(x_s,\lambda_s)| - \frac{1}{2\nu(x_s)}\right| \geq \varepsilon|\ln\varepsilon|\xi(\varepsilon),\ x_s \leq \frac{X_\delta^\varepsilon}{\varepsilon^2}\right) = 0.$$

Proof. This statement can be deduced from relation (7) and Lemma 4.2 which provides accurate estimates of f_L. ◻

6. Convergence of the coefficients of the soliton under the adiabatic approximation. Let us denote by Ω_L^ε the measurable subset of Ω defined by

$$\Omega_L^\varepsilon = \bigcup_{\delta>0}\{\omega \in \Omega \text{ such that } X_\delta^\varepsilon(\omega) \geq L\}.$$

We denote by ν^ε and μ^ε the rescaled processes defined on Ω_L^ε by $\nu^\varepsilon(x) = \nu(x/\varepsilon^2)$ and $\mu^\varepsilon(x) = \mu(x/\varepsilon^2)$ (i.e., the coefficients of the transmitted soliton in position x/ε^2) and on ${\Omega_L^\varepsilon}^c$ by $\nu^\varepsilon(x) = 0$ and $\mu^\varepsilon(x) = 0$. Z^ε is shorthand for the $\mathbb{R}^2$-valued process $(\nu^\varepsilon,\mu^\varepsilon)$.

PROPOSITION 6.1. *There exists a constant* K_δ *such that, for any* $\eta \in (0,1]$,

$$\limsup_{\varepsilon\to 0}\left|\mathbb{E}\left[Z^\varepsilon(x_\eta^\varepsilon) - Z^\varepsilon(x_0^\varepsilon) - \left(x_\eta^\varepsilon - x_0^\varepsilon\right)G(Z^\varepsilon(x_0^\varepsilon))/\mathcal{F}_0^{x_0^\varepsilon/\varepsilon^2}\right]\right| \leq K_\delta\eta^{3/2},$$

where $x_\eta^\varepsilon = (x_0+\eta)\wedge X_\delta^\varepsilon$ *and* G *is given by* (21).

Proof. The proof of this proposition is given in subsection 10.3. ◻

PROPOSITION 6.2. *Under the adiabatic approximation, the following assertions hold true for any $L > 0$.*

1. $\liminf_{\varepsilon\to 0} \mathbb{P}(\Omega_L^\varepsilon) = 1$.

2. *The $\mathbb{R}^2$-valued process $(\nu^\varepsilon(x), \mu^\varepsilon(x))_{x\in[0,L]}$ converges in probability in $\mathcal{C}^0$ to the $\mathbb{R}^2$-valued deterministic function $(\nu_l(x), \mu_l(x))_{x\in[0,L]}$ which satisfies system* (20).

Proof. Let $\delta > 0$ and denote by Z_δ^ε the stopped process

$$Z_\delta^\varepsilon(x) = Z^\varepsilon(x \wedge X_\delta^\varepsilon), \text{ for every } x \in [0, L].$$

$Z_l = (\nu_l, \mu_l)$ is the element of $\mathcal{C}^0$ given by (20). First, we show the tightness of Z_δ^ε in $\mathcal{C}^0$; second, we prove that there exists a unique weak limit for δ small enough.

Step 1. *Proof of tightness.* The tightness follows, on the one hand, from the fact that Z_δ^ε is uniformly bounded and, on the other hand, from (25), which imposes

$$|Z_\delta^\varepsilon(y) - Z_\delta^\varepsilon(x)| \le K_\delta |y - x| \text{ for any } 0 \le x \le y \le X_\delta^\varepsilon. \tag{30}$$

Step 2. *Proof of convergence.* Approximating the integral by the corresponding Riemann sum, we get from Proposition 6.1 that, for any function f in $\mathcal{C}_b^2(\mathbb{R}^2, \mathbb{R})$ and for any $0 \le x_0 \le x_1 \le L$,

$$\lim_{\varepsilon\to 0} \mathbb{E}\left[f(Z_\delta^\varepsilon(x_1)) - f(Z_\delta^\varepsilon(x_0)) - \int_{x_0\wedge X_\delta^\varepsilon}^{x_1\wedge X_\delta^\varepsilon} \mathcal{L}f(Z_\delta^\varepsilon(s))ds / \mathcal{F}_0^{x_0/\varepsilon^2} \right] = 0, \tag{31}$$

where $\mathcal{L} = G_1 \frac{\partial}{\partial\nu} + G_2 \frac{\partial}{\partial\mu}$ and G is given by (21). Denoting $\bar{Z}_\delta^\varepsilon(x) = Z_\delta^\varepsilon(x) - Z_l(x \wedge X_\delta^\varepsilon)$, applying (31) in the case where $x_0 = 0$ and $f(\nu, \mu) = \exp(-\nu^2 - \mu^2)$, we get that, for any x, $\lim_{\varepsilon\to 0} \mathbb{E}\left[f(\bar{Z}_\delta^\varepsilon(x))\right] = 1$. Since f takes the value 1 only in $(0, 0)$, we get that, for any $\delta < \delta(L) := \inf_{x\in[0,L]} \left\{\nu_l(x), \mu_l(x), \nu_l^{-1}(x), \mu_l^{-1}(x)\right\}$, we have $\limsup_{\varepsilon\to 0} \mathbb{P}(X_\delta^\varepsilon \le x) = 0$, which yields the first point of the proposition. Furthermore, this implies that, for any $\delta < \delta(L)$, for any bounded continuous functions $h_1, \dots, h_n$ and for any $0 \le y_1 < \cdots < y_n \le x_0$,

$$\lim_{\varepsilon\to 0} \mathbb{E}\left[h_1(Z_\delta^\varepsilon(y_1)) \dots h_n(Z_\delta^\varepsilon(y_n)) \left(f(Z_\delta^\varepsilon(x_1)) - f(Z_\delta^\varepsilon(x_0)) - \int_{x_0}^{x_1} \mathcal{L}f(Z_\delta^\varepsilon(s))ds \right) \right] = 0.$$

If we consider a subsequence ε_p such that $Z_\delta^{\varepsilon_p}$ weakly converges to some limit Z_δ, then we get [19] the following:

$$\mathbb{E}\left[h_1(Z_\delta(y_1)) \dots h_n(Z_\delta(y_n)) \left(f(Z_\delta(x_1)) - f(Z_\delta(x_0)) - \int_{x_0}^{x_1} \mathcal{L}f(Z_\delta(s))ds \right) \right] = 0,$$

which means that Z_δ is a solution of the martingale problem associated with the generator $\mathcal{L}$. This problem admits a unique solution which is the deterministic and continuous function Z_l. This consequently yields the second statement of the proposition. ∎

7. Asymptotic behavior of the transmitted soliton.

This section is devoted to the study of the asymptotic evolutions of the coefficients of the transmitted soliton as a function of the macroscopic length L of the random slab, i.e., L/ε^2 in the microscopic scale. By Proposition 6.2 these evolutions are given by (20). We aim to exhibit the relevant characteristics of this deterministic system of ordinary differential equations.

7.1. Limit behavior in the approximation $\nu_0 \ll \mu_0$. The system (20) can then be simplified to a good approximation:

$$
(32) \qquad \left\{ \begin{array}{ll} \dfrac{d\nu}{dL} = -\dfrac{d_1(4\mu)}{16}\dfrac{\nu}{\mu^2} - \dfrac{2d_2(4\mu)}{3}\dfrac{\nu^5}{\mu^2}, & \nu(0) = \nu_0, \\ \dfrac{d\mu}{dL} = -\dfrac{d_1(4\mu)}{48}\dfrac{\nu^2}{\mu^3} + \dfrac{18d_2(4\mu)}{35}\dfrac{\nu^6}{\mu^3}, & \mu(0) = \mu_0. \end{array} \right.
$$

It appears that $(1 - 1/3\ (\nu_0/\mu_0)^2)^{1/2} \leq \mu(L)/\mu_0 \leq (1 + 54/70(\nu_0/\mu_0)^2)^{1/2}$, which means that the velocity of the soliton is almost constant during the propagation, while the mass (equal to 4ν) decreases. Two cases can be distinguished depending on the value of the ratio $R = (32d_2(4\mu_0))/(3d_1(4\mu_0))$.

If $R\nu_0^4 < 1$, then the coefficient ν decreases exponentially with L:

$$
\nu(L) \simeq \nu_0 \exp\left(-\frac{L}{L_1}\right), \quad L_1 = \frac{16\mu_0^2}{d_1(4\mu_0)}.
$$

If $R\nu_0^4 > 1$, then the coefficient ν begins by decreasing as a power of L:

$$
\nu(L) \simeq \nu_0 \left(1 + \frac{L}{L_2}\right)^{-1/4}, \quad L_2 = \frac{3\mu_0^2}{8d_2(4\mu_0)\nu_0^4}.
$$

However, when ν becomes small enough, the decrease again has an exponential rate. The crossover between the power decay and the exponential decay occurs when $R\nu^4 \simeq 1$, i.e., when L reaches the value $L_3 = (R\nu_0^4 - 1)L_2$.

Remark 7.1. It can be noticed that, in the limit case $\nu_0/\mu_0 \to 0$, the incoming soliton can be approximated by a linear wavepacket

$$
u_0(t,x) \simeq \int_{-\infty}^{+\infty} dk\hat{\phi}_0(k)e^{ikx-ik^2t}, \text{ with } \hat{\phi}_0(k) = \frac{1}{2}\cosh^{-1}\left(\frac{\pi}{4}\left(\frac{k-2\mu_0}{\nu_0}\right)\right),
$$

whose spectrum $\hat{\phi}_0$ is sharply peaked about the wavenumber $k_0 = 2\mu_0$. Furthermore, the spectrum of the scattered wavepacket is peaked about the wavenumber $-2\mu_0$ (there exists also a secondary peak about $+2\mu_0$ which is much weaker). These statements are in agreement with the linear approximation. The localization length L_1, which can written in terms of the central wavenumber $L_1 = 4k_0^2/d_1(2k_0)$, corresponds to the localization length of a monochromatic wave with wavenumber k_0 scattered by a slab of linear random medium. In [2, Theorem 4.1], the authors show that in such a situation for ε small enough, the transmission coefficient T^ε satisfies with probability one

$$
\lim_{L\to\infty} \frac{1}{L}\ln|T^\varepsilon|^2(L) = -\frac{\varepsilon^2}{L_1} + O(\varepsilon^3).
$$

Remark 7.2. If the approximation $\nu \ll \mu$ holds for the initial conditions, then it actually holds true during the whole propagation, since the velocity is almost constant while the mass decreases. The domain $\nu \ll \mu$ is therefore stable.

7.2. Limit behavior in the approximation $\mu_0 \ll \nu_0$. The system (20) can then be simplified:

$$
(33) \qquad \left\{ \begin{array}{l} \dfrac{d\nu}{dL} = -\dfrac{\pi\sqrt{2}d_1(\nu^2\mu^{-1})}{2^8}\dfrac{\nu^{9/2}}{\mu^{11/2}}e^{-\frac{\pi}{2}\frac{\nu}{\mu}} - \dfrac{\pi\sqrt{2}d_2(\nu^2\mu^{-1})}{9.2^{12}}\dfrac{\nu^{25/2}}{\mu^{19/2}}e^{-\frac{\pi}{2}\frac{\nu}{\mu}}, \\ \dfrac{d\mu}{dL} = -\dfrac{\pi\sqrt{2}d_1(\nu^2\mu^{-1})}{2^9}\dfrac{\nu^{11/2}}{\mu^{13/2}}e^{-\frac{\pi}{2}\frac{\nu}{\mu}} - \dfrac{\pi\sqrt{2}d_2(\nu^2\mu^{-1})}{9.2^{13}}\dfrac{\nu^{27/2}}{\mu^{21/2}}e^{-\frac{\pi}{2}\frac{\nu}{\mu}}, \end{array} \right.
$$

with the initial conditions $\nu(0) = \nu_0$ and $\mu(0) = \mu_0$. It can be readily checked that $(1-2(\mu_0/\nu_0)^2)^{1/2} \le \nu(L)/\nu_0 \le 1$, which means that the mass of the soliton is almost constant during the propagation, while the velocity of the soliton decreases. The limit behavior for large L of the coefficient μ depends on the functions d_j—more exactly, on the high frequency behaviors of the Fourier transforms of the autocorrelation functions of the processes V_j. For instance, if $\mathbb{E}[V_j(0)V_j(t)] = \sigma_j^2\,(1-t/T_j)\,\mathbb{I}_{t\le T_j}$, then

$$\lim_{L\to\infty} \mu(L) \times \ln(L) = \frac{\pi\nu_0}{2},$$

which means that the velocity decreases as the logarithm of the length. This logarithmic rate actually represents the maximal decay of the velocity. Whatever the processes V_j, the terms of the right-hand sides of (33) have at least an exponential decay of the type $\exp -(\pi\nu)/(2\mu)$, which implies $\liminf_{L\to\infty} \mu(L) \times \ln(L) \ge \pi\nu_0/2$. However, the decay rate may be much slower. As an example, if the autocorrelation functions are $\mathbb{E}[V_j(0)V_j(t)] = \sigma_j^2 \exp(-t^2/T_j^2)$, then the velocity decreases as the square root of the logarithm of L:

$$\lim_{L\to\infty} \mu(L) \times \sqrt{\ln(L)} = \frac{\nu_0^2 \max(T_1, T_2)}{2}.$$

Remark 7.3. The approximation $\mu \ll \nu$ actually holds true during the whole propagation, since the mass is almost constant while the velocity decreases, which shows that the domain $\mu \ll \nu$ is stable.

7.3. Numerical integration of the asymptotic system. In the above paragraphs, we have exhibited two domains which are stable with respect to the evolutions of the coefficients of the transmitted soliton. We aim to show here that these regimes are not only stable but attractive. In order to prove this statement, we are going to solve numerically the system (20) for different values of the coefficients of the incoming soliton, without any assumption about the ratio of μ_0 to ν_0. For the sake of simplicity we choose to analyze the case where $V_2 \equiv 0$ and V_1 admits an autocorrelation function with compact support:

$$\mathbb{E}[V_1(0)V_1(t)] = \frac{1}{12}\,(1-t)\,\mathbb{I}_{t\le 1}.$$

Figures 2 and 3 plot the evolutions of the coefficients of the transmitted soliton as functions of the length of the random slab. The mass N_0 is chosen at some fixed value for all figures, equal to 2, but the initial velocity V_0 varies from 0.8 to 3.2. The striking point is that two different behaviors are found and that they are separated from each other by a critical value V_c of the initial velocity V_0.

When $V_0 > V_c$ (Figure 2), after a transition regime where the mass decreases as a power, the velocity reaches a stable value $V_{\lim}$. This limit value is very close to the initial value V_0 when $V_0 \gg V_c$. Once the velocity is stable, the mass decreases exponentially with the localization length $V_{\lim}^2/d_1(V_{\lim})$; this regime has been described in subsection 7.1.

When $V_0 < V_c$ (Figure 3), after a transition regime where both the mass and velocity decrease, the mass reaches a stable value $N_{\lim}$, which is close to the initial mass N_0 if $V_0 \ll V_c$. Once the mass is stable, the velocity decreases as $(\pi N_{\lim})/(2\ln L)$, as described in subsection 7.2. The two small figures evidently show that the mass is conserved over very large distances and that the decrease of the velocity is very slow.

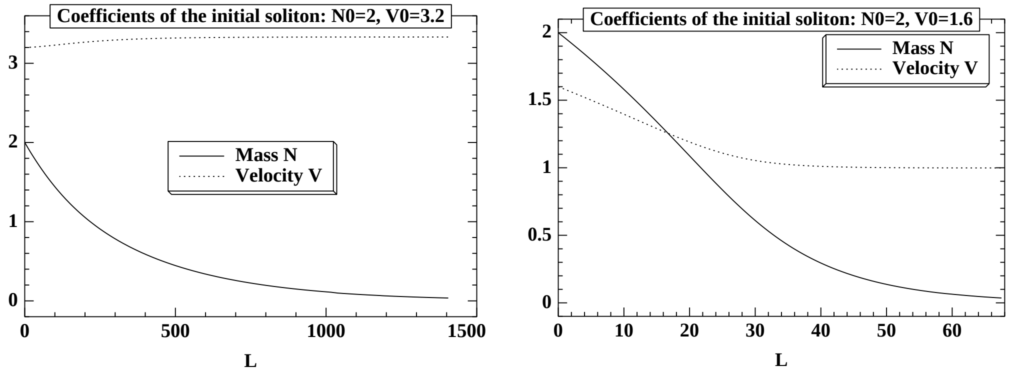

FIG. 2. *Coefficients of the transmitted soliton, with the initial velocity* $V_0 > V_c$.

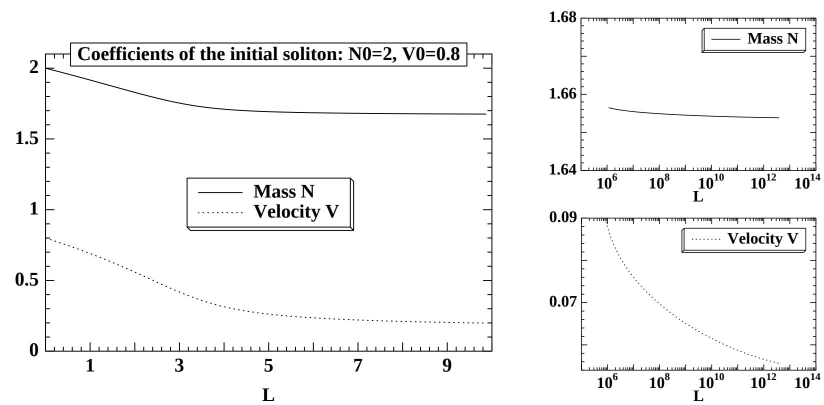

FIG. 3. *Coefficients of the transmitted soliton, with the initial velocity* $V_0 < V_c$.

Numerically the critical value V_c of the velocity which separates the two regimes described above is found to be about 1.39 with the perturbation model and the initial mass which have been adopted (data not shown). If we choose another model or else a different value of the initial mass, then we find the same kinds of behaviors, but the value of the critical velocity V_c is shifted. One can also notice that the critical point V_c is unstable. Practically we always observe one of the limit behaviors described in the subsections 7.1 and 7.2.

8. Accuracy of the adiabatic approximation. We aim to show in this section that the adiabatic approximation can be a posteriori verified. This verification will consist of proving that the scattered wavepacket which has been determined above has actually no noticeable influence on the evolutions of the Jost coefficients a and b. We are going to study the components which have been neglected until now and which are related to the interplay between the soliton and the scattered wavepacket on the one hand, and which are due to the sole effect of the scattered wavepacket on the other hand. The functions γ (resp., $\bar{\gamma}$) given by (19) can be split into the sum $\gamma_L + \gamma_{NL}$ (resp., $\bar{\gamma}_L + \bar{\gamma}_{NL}$), where γ_L (resp., $\bar{\gamma}_L$) originates from the perturbation of the linear potential V_1 and γ_{NL} (resp., $\bar{\gamma}_{NL}$) originates from the perturbation of the nonlinear index of refraction V_2.

8.1. Components of the functions $\gamma_{NL}$and $\bar{\gamma}_{NL}$. We shall first deal with the components associated with the functions γ_{NL} and $\bar{\gamma}_{NL}$. We can find two kinds of terms. In the first kind there is a term u_S or f_{1S} which originates from the soliton in the integrated expression (19). The presence of $\cosh(2\nu(x-x_s))$ in the denominator then involves this term localizing about the center of the soliton x_s. In the second kind, all terms u or f_1 originate from the scattered wavepacket. The integrand is not localized anymore. The so-called "degree" of a component, that is to say the number of terms in the integrand of (19) which originate from the scattered wavepacket, then appears to be a key parameter.

Localized components of degree 1 *of the functions* γ_{NL} *and* $\bar{\gamma}_{NL}$. Let us fix λ and consider one of the components:

$$\gamma_A(x_s) = \int dx V_2(x)|u_S|^2 u_L^* f_{2S}^2.$$

Substituting for u_S, f_{2S}, and u_L their calculated expressions, we find that $\gamma_A(x_s)$ is a sum of terms of the type ($q \geq 1$):

$$\varepsilon^2 \int_0^{L/\varepsilon^2} dx V_2(x) e^{2i\lambda x} R_1(\nu(x),\mu(x),\lambda) \frac{\tanh^p(2\nu(x)(x-x_s))}{\cosh^q(2\nu(x)(x-x_s))}$$
$$\times \int_0^{x_s} dy V_j(y) \int_{-\infty}^{+\infty} d\lambda' R_2^* c_j^*(\nu(y),\mu(y),\lambda') e^{i(-2\lambda' x + 4\lambda'^2 t_s(x))} e^{-i\psi_s(y,\lambda')},$$

where ψ_s is given by (24) and R_j, $j=1,2$ are rational functions without any pole over the real axis λ and uniformly bounded with respect to $(\mu,\nu,\lambda) \in D_\delta \times \mathbb{R}$ by a constant which depends only on δ. We denote by A^ε the integral with respect to x_s of $\gamma_A^*(x_s) e^{4i\lambda^2 t_s(x_s)}$ over the interval $[0, L/\varepsilon^2)$. We then find, by using tabulated formulae [7, Formula 3.512],

$$A^\varepsilon = \varepsilon^2 C_{p,q} \int_0^{L/\varepsilon^2} dx V_2(x) \frac{R_1^*(\nu(x),\mu(x),\lambda)}{2\nu(x)} e^{-2i\lambda x + 4\lambda^2 t_s(x)} \int_0^x dy V_j(y) \xi_2(x,y),$$

where $\xi_2(x,y) = \int_{-\infty}^{+\infty} d\lambda' R_2 c_j(\nu(y),\mu(y),\lambda') e^{i(2\lambda' x - 4\lambda'^2 t_s(x) + \psi_s(y,\lambda'))}$ and the value of $C_{p,q}$ is given by the beta function $B(\frac{p+1}{2},\frac{q}{2})$ [7]. A sharp study of A^ε which relies on the same kind of estimates as the proof of Lemma 4.2 then proves that [6]

$$\limsup_{\varepsilon\to 0} \mathbb{E}\left[|A^\varepsilon|^2 \mathbb{I}_{\Omega_L^\varepsilon}\right] = 0.$$

Since $\mathbb{P}(\Omega_L^\varepsilon) \to 1$, this yields that the influence of γ_A on the evolutions of the Jost coefficients is negligible.

Localized components of higher degree of the functions γ_{NL} *and* $\bar{\gamma}_{NL}$. Let us consider, for instance, the component

$$\gamma_B(x_s) = \int dx V_2(x)|u_L|^2 u_S^* f_{2S}^2.$$

We could achieve a study similar to that of γ_A. However, a direct estimate is sufficient here. Indeed, since u_L is of order $\varepsilon|\ln\varepsilon|$ and the integrand inside γ_B is localized, γ_B is of order $\varepsilon^2|\ln\varepsilon|^2$. From (18), the variations of the Jost coefficients over an interval of order 1 are of order $\varepsilon\gamma$, i.e., of order $\varepsilon^3|\ln\varepsilon|^2$. Since this variation is integrated over a slab of length L/ε^2, we finally get that the total variations of the Jost coefficients due to γ_B are of order $\varepsilon|\ln\varepsilon|^2$, which is negligible.

Nonlocalized components of the functions γ_{NL} and $\bar{\gamma}_{NL}$. One of these components is, for instance,

$$\gamma_C(x_s) = -\int dx V_2(x)|u_L|^2 u_L f_1{}_L^2.$$

The integrand is not localized about the center of the soliton, but is the product of functions u_L and f_L which are small and are of order $\varepsilon|\ln\varepsilon|$. Since $|u|^2 u f_1$ can be put into factor, it follows that γ_C is of order $\varepsilon^2|\ln\varepsilon|^4$. Thus the variations of the Jost coefficients due to this term over an interval of order 1 are of order $\varepsilon^3|\ln\varepsilon|^4$, and the total variations of the Jost coefficients are at most of order $\varepsilon|\ln\varepsilon|^4$.

Unfortunately there exists a term which does not fulfill the above conditions,

$$\gamma_D(x_s) = \int dx V_2(x)|u_L|^2 u_L^* f_2{}_S^2,$$

because f_{2S} is not localized. By using a direct estimate we find that γ_D is of order $\varepsilon|\ln\varepsilon|^3$ and could have an influence of order 1 on the total variations of the Jost coefficients. A sharp study similar to that of γ_A can be achieved to prove that the influence of γ_D is actually small.

Conclusion. If $V_1 \equiv 0$, which means that only the nonlinear coefficient is randomly perturbed, then the adiabatic approximation is justified. Physically speaking, the soliton emits quasi-linear waves of small amplitude $\sim \varepsilon$. Since the perturbation is of the type $\varepsilon V_2|u|^2 u$, its influence on the linear waves is much smaller, with a ratio of order ε^3, than the other terms of the Schrödinger equation. As a consequence the scattered waves do not feel the perturbation V_2, even on a slab of order ε^{-2}, and propagate as if they were in homogeneous space. Once they have been generated, they do not affect the further evolution of the soliton. That is why the adiabatic approximation is physically reasonable.

8.2. Components of the functions $\gamma_L$and $\bar{\gamma}_L$. We assume here that $V_1 \neq 0$ and we consider the components of the functions γ_L and $\bar{\gamma}_L$. The above analysis of the functions γ_{NL} and $\bar{\gamma}_{NL}$ still holds true for some of the components of γ_L and $\bar{\gamma}_L$, but fails for some others. It seems that some of these components involve modifications of order 1 of the Jost coefficients. In fact this is unavoidable. The scattered waves are of linear type, and V_1 is a perturbation of the linear potential. It is well known about the linear Schrödinger equation with random potential of order ε that wavepackets are affected for slabs of order ε^{-2} [15]. So we cannot expect to show that the scattered wavepacket will not affect the evolutions of the Jost coefficients. However, we may think that the adiabatic approximation still holds true in the following sense. Since V_1 is a perturbation of the *linear* potential, the primary effects of the components of the functions γ_L and $\bar{\gamma}_L$ associated with the scattered wavepacket concern only the wavepacket itself. If such modifications do not qualitatively affect its nature, the interplay between the scattered wavepacket and the soliton may not be affected and may still be considered as negligible. We can therefore expect that the scattered wavepacket has no influence on the evolution of the soliton. Nevertheless, the proof of this assertion has not yet been completed.

Conclusion. If $V_1 \neq 0$, the adiabatic approximation is to be justified. The following section presents numerical results which indicate that this approximation should actually be accurate.

9. Numerical simulations. The results in the previous sections are theoretically valid in the limit case $\varepsilon \to 0$, where the amplitudes of the perturbations go to zero and the length of the random slab goes to infinity. In this section we aim to show that the asymptotic behaviors of the soliton can be observed in numerical simulations in the case where ε is small; more precisely, smaller than any other characteristic scale of the problem. We use a fourth-order split-step method to simulate the perturbed nonlinear Schrödinger equation (14). This numerical algorithm provides accurate and stable solutions to a large class of nonlinear partial differential equations [13].

Let Δt be the elementary time step and h be the elementary space step. We denote by $\left(u^0(jh)\right)_{j=-K,\ldots,K-1}$ the initial wave solution. By induction we compute $u^{n+1} := \left(u((n+1)\Delta t, jh)\right)_{j=-K,\ldots,K-1}$ from $u^n := \left(u(n\Delta t, jh)\right)_{j=-K,\ldots,K-1}$:

$$\begin{aligned} \text{first step:} \quad & u^{n+1/3} = A(\Delta t/2)u^n, \\ \text{second step:} \quad & u^{n+2/3} = B(\Delta t)u^{n+1/3}, \\ \text{third step:} \quad & u^{n+1} = A(\Delta t/2)u^{n+2/3}, \end{aligned}$$

where $A(\Delta t/2)$ is the linear operator generated by $i\frac{\partial^2}{\partial x^2}$ and B is simply a scalar multiplication in the physical space by $\exp i\left((2-\varepsilon V_2)|u|^2 - \varepsilon V_1\right)\Delta t$. The first and third steps can be solved using a Fourier transform. Indeed, in Fourier space the effect of the exponential operator $A(\Delta t/2)$ is a scalar multiplication by $\exp -i(k^2\Delta t/2)$. To sum up, the split step algorithm involves a sequence of steps that include free-space propagation over a half-step, then a nonlinear correction, and free-space propagation over the final half-step. Practically, it is easy to see that the two back-to-back free-space half-steps can be combined into a single free-space step over Δt. The error of the split-step algorithm comes from the splitting process, because the operators A and B do not commute. It is well known that the method described above is of second order [18]. However, since the NLS equation is time reversible, we can use a standard method which transforms a second-order method into a fourth-order method [21]. Indeed, if $C(\Delta t)u(t,x)$ is a second-order approximation to $u(t+\Delta t, x)$, then $C(\alpha\Delta t)C(-\beta\Delta t)C(\alpha\Delta t)u(t,x)$ is a fourth-order approximation to $u(t+\Delta t, x)$, if we take care to choose $\alpha = 1/(2-2^{1/3})$ and $\beta = 2^{1/3}/(2-2^{1/3})$. The drawback of this method is that we implicitly impose periodicity on the solutions because of the Fourier transform that is used on a finite interval. We can control it by using a shifting computational domain which is always at the center of the mass of the solution. Moreover we shall impose boundaries of this domain that absorb outgoing waves. This can be readily achieved by adding a complex potential which is smooth so as to reduce reflections. We choose to substitute the complex potential $V(x) = V_1(x) - iV_{abs}(x)$ for the random potential $V_1(x)$:

$$V_{abs}(x) = \begin{cases} V_{abs\max}\sin^2\left(\dfrac{\pi}{2}\dfrac{x_l - x}{x_l - X_l}\right), & \text{if } X_l \le x < x_l, \\ 0 & \text{if } x_l \le x < x_r, \\ V_{abs\max}\sin^2\left(\dfrac{\pi}{2}\dfrac{x - x_r}{X_r - x_r}\right) & \text{if } x_r \le x < X_r, \end{cases}$$

where X_l (resp., X_r) is the left (resp., right) end of the computational domain, and $[X_l, x_l]$ (resp., $[x_r, X_r]$) is the left (resp., right) absorbing slab. The energy (or Hamiltonian) defined by (15) is theoretically preserved by the split-step method up to the machine accuracy in case of a truly periodic situation without absorption. The domain that we consider is not periodic, since it shifts along the simulation and the outgoing wave is absorbed by an imaginary potential at the boundaries of the domain. However, the size of the shifting domain is taken so that the distortion imposed by the

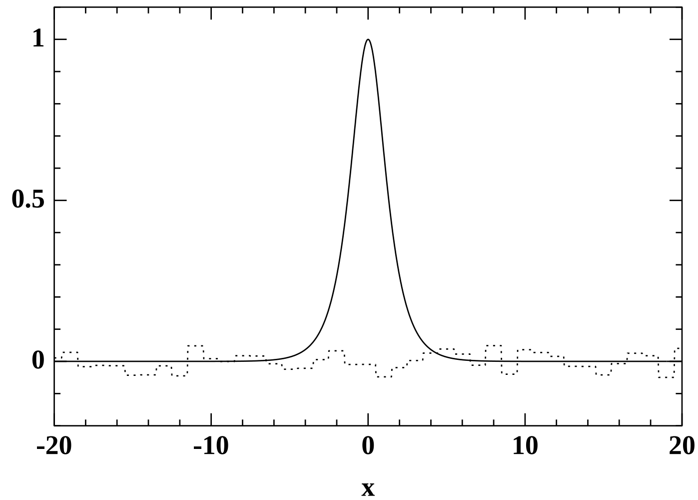

FIG. 4. *Envelope of the initial soliton (solid line) whose mass is* $N_0 = 2$ *and velocity* $V_0 = 1.6$*. The dashed line plots the profile of one realization of the random potential* εV_1 *with* $\varepsilon = 0.1$*.*

nonperiodicity has a negligible effect. We adopt in this section the following model for the linear random potential:

$$V_1(x) = A_l \text{ if } l + X_0 \leq x < l + X_0 + 1,$$

where $(A_l)_{l=0,\dots,L-1}$ is a sequence of independent and identically distributed variables, which obey uniform distributions over the interval $[-1/2, 1/2]$, and X_0 is a random variable independent of $A_.$ which also obeys a uniform distribution over $[-1/2, 1/2]$. The autocorrelation function of the ergodic process V_1 is equal to $\mathbb{E}[V_1(0)V_1(t)] = \frac{1}{12}(1-t)\,\mathbb{I}_{t\leq 1}$ as in subsection 7.3. For simplicity we also take $V_2 \equiv 0$. The integer L which is equal to the length of the random slab will be chosen so large that we can observe the effect of the small perturbation εV_1. We measure the mass (i.e., the L^2-norm) and center of the solution during the propagation, and also the envelope of the transmitted solution, so that we can compare them with the envelope of the incident soliton. The mass $N(n\Delta t)$ and the center $C(n\Delta t)$ are computed at time $n\Delta t$ from the data $(u(n\Delta t, jh))_{j=-K,\dots,K-1}$ as

$$N(n\Delta t) = h \times \sum_{j=-K}^{K-1} |u(n\Delta t, jh)|^2, \quad C(n\Delta t) = h \times \sum_{j=-K}^{K-1} |u(n\Delta t, jh)|^2 j / N(n\Delta t).$$

We finally deal with the set of data $(C(n\Delta t))_n$ in order to compute the velocity of the solution, defined here as the time-derivative of the center. We present 10 simulations where the initial wave at time $t = 0$ is a soliton with mass $N_0 = 2$ and velocity $V_0 = 1.6$ centered at $x = 0$. In the first we simulate the homogeneous nonlinear Schrödinger equation (2), which admits as an exact solution (12). We can therefore check the accuracy of the numerical method, since we can see that the computed solution maintains a very close resemblance to the initial soliton (data not shown), while the mass and velocity are almost constant (thin solid lines of Figure 5). The nine other simulations are carried out with nine different realizations of the random potential with $\varepsilon = 0.1$ (see Figure 4). The simulated evolutions of the coefficients of

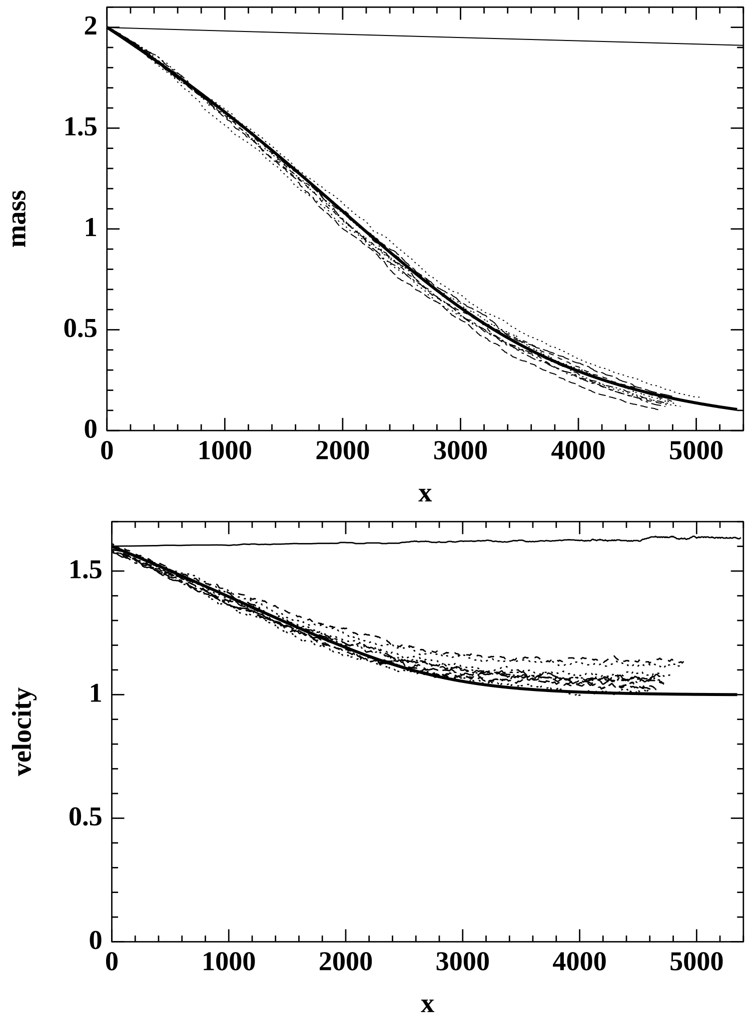

FIG. 5. *Coefficients of the transmitted soliton whose initial coefficients are $N_0 = 2$, $V_0 = 1.6$ with a random potential whose amplitude is $\varepsilon = 0.1$. The upper (resp., lower) figure is devoted to the mass (resp., velocity). The thick solid lines represent the theoretical coefficients of the transmitted soliton. The thin solid lines plot the simulated coefficients of the soliton when no random potential is present. The thin dashed and dotted lines plot the simulated masses and velocities of the transmitted solitons for nine different realizations of the random potential.*

the soliton are presented in Figure 5 and compared with the theoretical evolutions given by (20) in the scale x/ε^2. It thus appears that the numerical simulations are in very good agreement with the theoretical results. The simulated masses follow the theoretical ones very closely. This is partly due to the fact that the split-step method preserves the total mass

$$N_{tot} = 4\nu + \int_{-\infty}^{\infty} n(\lambda) d\lambda. \tag{34}$$

This implies stability for the coefficient ν and the mass of the soliton. The results may seem a bit less convincing when one looks at the velocity. Indeed, the split-step

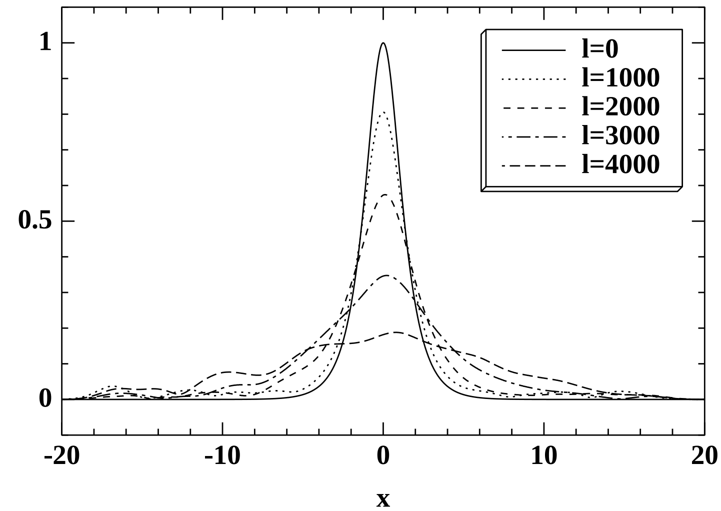

FIG. 6. *Envelopes of the soliton when its center crosses different depth lines l for one of the realizations of the random potential with an amplitude equal to $\varepsilon = 0.1$. The coordinate x is normalized around the depth line l. The initial wave is a soliton with mass $N_0 = 2$ and velocity $V_0 = 1.6$.*

method preserves the total energy which can be expressed from (11) and (15) as

$$E_{tot} = 16\left(\nu\mu^2 - \frac{\nu^3}{3}\right) + 4\int_{-\infty}^{\infty} \lambda^2 n(\lambda) d\lambda + \int \varepsilon V_1(x)|u|^2 + \frac{\varepsilon}{2} V_2(x)|u|^4 dx. \tag{35}$$

The two last terms are negligible in the asymptotic framework $\varepsilon \to 0$, but when $\varepsilon = 0.1$, they give rise to local fluctuations of the coefficient μ and of the instantaneous velocity of the soliton. The velocities plotted in Figure 5 have actually been smoothed by averaging over intervals of length $\Delta x_{ave} = 20$. This instability could explain the slight dispersal of the lines plotting the simulated velocities. Figure 6 plots the envelopes of the solution at different depths corresponding to one of the simulations, which shows that the wave keeps the basic form of a soliton although it loses some mass. In [6] more numerical simulations are presented, where we test different values for the coefficients of the initial soliton and different models for the random fluctuations of the linear potential V_1 and the nonlinear index of refraction V_2. All these results confirm that system (20) accurately describes the transmission of a soliton through a random slab for small perturbations and long slab length.

10. Technical estimates.

10.1. Proof of Lemma 4.2. Let us fix a function P of class $\mathcal{C}^2$ with polynomial growth and a point $x_s \in [0, L \wedge X_\delta^\varepsilon/\varepsilon^2]$. From Proposition 4.1 we can deduce that Q^ε is equal to the sum $Q_1^\varepsilon + Q_2^\varepsilon$:

$$Q_j^\varepsilon(x_s) = \varepsilon \int_0^{x_s} dx V_j(x) \int d\lambda P_j(x,\lambda) e^{i\left(2\lambda(y-x)+\lambda^2\kappa(x)+\phi_s(x)\right)},$$

where $\kappa(x) = 4(t_s(x) - t_s(x_s))$, $P_j(x,\lambda) = P(\lambda)c_j(\nu(x),\mu(x),\lambda)$ and $c_j(\nu,\mu,\lambda)$ is given by (22). Let us fix $j = 1$ or 2. By ordering the terms in the exponential with respect to their λ-powers, then centering the integral with respect to λ about the central value, we obtain $Q_j^\varepsilon(x_s) = Q_{j\,A}^{\,\varepsilon}(x_s) + Q_{j\,B}^{\,\varepsilon}(x_s)$:

$$Q_{j\,A,B}^{\,\varepsilon}(x_s) = \varepsilon \int_0^{x_s} dx V_j(x)\xi_{j\,A,B}(x) e^{i\left(-(x-y)^2/\kappa(x)+\phi_s(x)\right)}, \tag{36}$$

where $\xi_{j\,A}$ and $\xi_{j\,B}$ are given by

$$\xi_{j\,A}(x) = \int_{-\infty}^{+\infty} d\lambda \left(P_j\left(x, \lambda + \chi(x)\right) - P_j\left(x, \chi(x)\right)\right) e^{i\kappa(x)\lambda^2}, \quad \xi_{j\,B}(x) = C\frac{P_j\left(x, \chi(x)\right)}{\sqrt{\kappa(x)}},$$

with $\chi(x) = (x-y)/\kappa(x)$ and $C = \int_{-\infty}^{+\infty} d\lambda e^{i\lambda^2} = e^{i\pi/4}\sqrt{\pi}$. We first deal with $Q_{j\,A}$ and estimate $\xi_{j\,A}$. We write $P_j(x, \lambda+\chi) - P_j(x,\chi) = \int_0^\lambda P_j'(x, s+\chi)ds$. Then we exchange the order of the integrals with respect to λ and s in the expression of $\xi_{j\,A}$:

$$\xi_{j\,A}(x) = \int_{-\infty}^{\infty} ds P_j'(x, s+\chi(x))\mathrm{sgn}(s)\frac{\gamma(|s|\sqrt{|\kappa(x)|})}{\sqrt{|\kappa(x)|}}, \text{ where } \gamma(s) = \int_s^{+\infty} d\lambda e^{i\lambda^2}.$$

Writing $P_j'(x, s+\chi) = \int_{-\infty}^s du P_j''(x, u+\chi)$ for $s \le 0$ and $P_j'(x, s+\chi) = -\int_s^\infty du P_j''(x, u+\chi)$ for $s > 0$, and exchanging the integrals with respect to s and u, yields

$$\left|\xi_{j\,A}(x)\right| \le \int_{-\infty}^{\infty} du \frac{|P_j''(x, u+\chi(x))|}{|\kappa(x)|} \times 2\sup_{v\ge 0}\left|\int_0^v ds\gamma(s)\right|.$$

A short study of the tails of the Fresnel cosine and sine establishes that the primitive function of γ is uniformly bounded with respect to $v \ge 0$ by $1+\pi$. Since the second λ-derivative of P_j belongs to L^1 uniformly with respect to x, we then get that there exists a constant K_δ such that $|\xi_{j\,A}(x)| \le K_\delta/|\kappa(x)| \sim |x-x_s|^{-1}$ as $|x-x_s| \to \infty$ almost surely. Besides, $\xi_{j\,A}$ is uniformly bounded since P_j belongs to L^1 uniformly with respect to x. Injecting into (36) and taking into account the fact that $x_s \sim \varepsilon^{-2}$, we get

$$\left|Q_{j\,A}^{\,\varepsilon}(x_s)\right| \le K_\delta \varepsilon |\ln \varepsilon|. \tag{37}$$

We aim now to estimate $Q_{j\,B}^{\,\varepsilon}$. We fix a real $M > 0$ and introduce

$$Q_{j\,B}^{\,\varepsilon,M}(x_s) = \varepsilon \int_0^{x_s} dx V_j(x)\xi_{j\,B}^{\,M}(x) e^{i\left(-(x-y)^2/\kappa^M(x)+\phi_s^M(x)\right)},$$

where

$$\phi_s^M(x) = \phi_s((x-M)^+) + (x-(x-M)^+)(\mu^2+\nu^2)/\mu((x-M)^+),$$
$$\kappa^M(x) = \kappa((x-M)^+) + (x-(x-M)^+)/\mu((x-M)^+),$$

and

$$\xi_{j\,B}^{\,M}(x) = CP_j((x-y)/\kappa^M(x), (x-M)^+)/\sqrt{|\kappa^M(x)|}.$$

We can note that $|\mu((x-M)^+) - \mu(x)| \le K_\delta\varepsilon^2 M$, $|\nu((x-M)^+) - \nu(x)| \le K_\delta \varepsilon^2 M$, $|\kappa_M(x) - \kappa(x)| \le K_\delta\varepsilon^2 M^2$, and $|\phi_s(x) - \phi_s^M(x)| \le K_\delta \varepsilon^2 M^2$ uniformly with respect to x. Also taking into account the fact that $\xi_{j\,B}$ and $\xi_{j\,B}^{\,M}$ decay as $|x-x_s|^{-1/2}$, we then find that there exists a constant K_δ such that

$$\left|Q_{j\,B}^{\,\varepsilon,M}(x_s) - Q_{j\,B}^{\,\varepsilon}(x_s)\right| \le K_\delta \varepsilon^2 M^2. \tag{38}$$

On the other hand, since ${\xi_j}_B^M(x)$, $\phi_s(x-M)$, and $\kappa^M(x)$ are $\mathcal{F}_0^{x-M}$-measurable, we can apply the mixing property of the process V_j and Lemma 10.4 to establish that

$$\mathbb{E}\left[\left|{Q_j}_B^{\varepsilon,M}(x_s)\right|^2 \mathbb{I}_{x_s\le X_\delta^\varepsilon/\varepsilon^2}\right] \le K_\delta\left(\varepsilon^2|\ln\varepsilon| + \phi(M)\right), \tag{39}$$

where $M \mapsto \phi(M)$ is the mixing function of V_j, which decays at least as M^{-4}. Optimizing the sum of (37), (38), and (39) by choosing $M = \varepsilon^{-1/2}$, we get the desired result.

10.2. Estimates of the scattered wavepacket. Let us introduce the quantity $n(t/\varepsilon^2,\lambda) := -\pi^{-1}\ln|a(t/\varepsilon^2,\lambda)|^2$. The spectral parameter λ is proportional to the wavenumber k of the generated radiation: $k = 2\lambda$ [17], so that $n(\lambda)$ is the spectral density of scattered mass at frequency 2λ.

LEMMA 10.1. 1. *Under the adiabatic approximation, if $t \le t' \le T_\delta^\varepsilon$, then*

$$\left|\Delta n(\lambda) - \frac{1}{\pi}\left|\frac{\bar b}{a}\left(\frac{t'}{\varepsilon^2},\lambda\right) - \frac{\bar b}{a}\left(\frac{t}{\varepsilon^2},\lambda\right)\right|^2\right| \le \frac{1}{2\pi}\left|\frac{\bar b}{a}\left(\frac{t'}{\varepsilon^2},\lambda\right) - \frac{\bar b}{a}\left(\frac{t}{\varepsilon^2},\lambda\right)\right|^4,$$

where $\Delta n(\lambda) = n(t'/\varepsilon^2,\lambda) - n(t/\varepsilon^2,\lambda)$.

2. *If $t \le t' \le T_\delta^\varepsilon$, then there exists a constant K_δ such that the variations of the coefficients of the soliton can be estimated by*

$$\nu\left(\frac{t'}{\varepsilon^2}\right) - \nu\left(\frac{t}{\varepsilon^2}\right) = -\frac{1}{4}\Delta n_0,$$

$$\left|\mu\left(\frac{t'}{\varepsilon^2}\right) - \mu\left(\frac{t}{\varepsilon^2}\right) + \frac{1}{8\mu\nu}\left(\frac{t}{\varepsilon^2}\right)\Delta n_2 + \left(\frac{\nu}{8\mu} - \frac{\mu}{8\nu}\right)\left(\frac{t}{\varepsilon^2}\right)\Delta n_0\right| \le K_\delta\left(\varepsilon + |\Delta n_0|^2 + |\Delta n_2|^2\right),$$

where $\Delta n_j = \int_{-\infty}^{+\infty}\lambda^j\Delta n(\lambda)d\lambda$ for $j = 0, 2$.

Proof. The first point can be readily deduced from the definition of n. On the other hand, since the total mass (34) is a conserved quantity, we can deduce the variation of the coefficient ν. Finally the total energy E_{tot} given by (35) is preserved, and the last two terms of the energy (35) are of order ε, since V_1 and V_2 belong to L^∞ while the L^2- and L^4-norms of u are uniformly bounded by Lemma 3.1. Some simple manipulations then yield the variation of the coefficient μ. ∎

10.3. Proof of Proposition 6.1. We denote $g(\nu,\mu,\lambda) = -4G_1(\nu,\mu,\lambda)$ which is a positive function. If $x \le X_\delta^\varepsilon$, then $g(x/\varepsilon^2,\lambda)$ is shorthand for $g(\nu(x/\varepsilon^2),\mu(x/\varepsilon^2),\lambda)$. Let us fix x_0. We recall that $x_\eta^\varepsilon = (x_0+\eta)\wedge X_\delta^\varepsilon$. By (30) we can choose η small enough so that $|Z^\varepsilon(x) - Z^\varepsilon(x_0^\varepsilon)| \le \eta^{1/2}$ for every $x \in [x_0^\varepsilon, x_\eta^\varepsilon]$. We denote by $n(x_0^\varepsilon, x_\eta^\varepsilon,\lambda)$ the density of mass scattered by the soliton over the interval $[x_0^\varepsilon/\varepsilon^2, x_\eta^\varepsilon/\varepsilon^2]$. We introduce the approximate density $\bar n_\eta^\varepsilon(\lambda)$ defined by

$$\bar n_\eta^\varepsilon(\lambda) = \frac{\varepsilon^2}{\pi}\left|\sum_{j=1}^2\int_{x_0^\varepsilon/\varepsilon^2}^{x_\eta^\varepsilon/\varepsilon^2} c_j(\nu(x),\mu(x),\lambda)e^{i(\phi_s(x)-2\lambda x+4\lambda^2 t_s(x))}V_j(x)dx\right|^2.$$

It will appear in the following that $\bar n_\eta^\varepsilon(\lambda)$ is an accurate approximation of $n(x_0^\varepsilon, x_\eta^\varepsilon,\lambda)$. We also introduce the auxiliary density $\tilde n_\eta^\varepsilon$ defined by

$$\tilde n_\eta^\varepsilon(\lambda) = \frac{\varepsilon^2}{\pi}\left|\sum_{j=1}^2\int_{x_0/\varepsilon^2}^{(x_0+\eta)/\varepsilon^2}\tilde c(x,\lambda)V_j(x)dx\right|^2,$$

where $\tilde{c}(x,\lambda) = c_j(\tilde{\nu}(x), \tilde{\mu}(x), \lambda)e^{i(\tilde{\phi_s}(x)-2\lambda x+4\lambda^2\tilde{t_s}(x))}$, $\tilde{\nu}(x) = \nu(x \wedge x_\eta^\varepsilon/\varepsilon^2)$, $\tilde{\mu}(x) = \mu(x \wedge x_\eta^\varepsilon/\varepsilon^2)$, and $\tilde{\phi_s}$ and $\tilde{t_s}$ are given by

$$\frac{d\tilde{\phi_s}}{dx} = \frac{\tilde{\mu}^2+\tilde{\nu}^2}{\tilde{\mu}} \text{ if } x \geq \frac{x_\eta^\varepsilon}{\varepsilon^2}, \quad \tilde{\phi_s}(x) = \phi_s(x) \text{ if } x \leq \frac{x_\eta^\varepsilon}{\varepsilon^2},$$
$$\frac{d\tilde{t_s}}{dx} = \frac{1}{4\tilde{\mu}} \text{ if } x \geq \frac{x_\eta^\varepsilon}{\varepsilon^2}, \qquad \tilde{t_s}(x) = t_s(x) \text{ if } x \leq \frac{x_\eta^\varepsilon}{\varepsilon^2}.$$

In particular, the processes $\tilde{(.)}$ are equal to the processes $(.)$ while $x \leq x_\eta^\varepsilon/\varepsilon^2$, and they are $\mathcal{F}_0^{x\wedge x_\eta^\varepsilon/\varepsilon^2}$-measurable. The proof of Proposition 6.1 requires the following lemmas, whose proofs will be sketched. The interested reader is referred to [6] for a complete study.

LEMMA 10.2. *There exists constants K_δ and $C_\delta > 0$ such that, for any λ and $\eta \in (0,1)$,*

$$\left|\mathbb{E}\left[\bar{n}_\eta^\varepsilon(\lambda) - \tilde{n}_\eta^\varepsilon(\lambda)/\mathcal{F}_0^{x_\eta^\varepsilon/\varepsilon^2}\right] - (x_0+\eta-x_\eta^\varepsilon)g(x_\eta^\varepsilon/\varepsilon^2,\lambda)\right| \leq K_\delta e^{-C_\delta\lambda^2}\varepsilon.$$

Proof. This result follows from the mixing property of the process V_j and the fact that all terms except $V_j(x)$ are $\mathcal{F}_0^{x_\eta^\varepsilon/\varepsilon^2}$-measurable in the integrand of the integral that defines $\tilde{n}_\eta^\varepsilon(\lambda)$. □

LEMMA 10.3. *There exists constants $C_\delta > 0$ and K_δ such that, for any λ and $\eta \in (0,1)$,*

$$\limsup_{\varepsilon\to 0}\left|\mathbb{E}\left[\tilde{n}_\eta^\varepsilon(\lambda) - \eta g(x_0/\varepsilon^2,\lambda)/\mathcal{F}_0^{x_0/\varepsilon^2}\right]\mathbb{I}_{x_0\leq X_\delta^\varepsilon}\right| \leq K_\delta\eta^2 e^{-C_\delta\lambda^2}.$$

Proof. Rewriting $\tilde{n}_\eta^\varepsilon(\lambda)$ as a double integral, denoting $\nu = \nu(x_0/\varepsilon^2)$, $\mu = \mu(x_0/\varepsilon^2)$, $\hat{c}(x,\lambda) = c_j(\nu,\mu,\lambda)e^{ik(\nu,\mu,\lambda)x}$, and using (25), we find that

$$\left|\mathbb{E}\left[\tilde{n}_\eta^\varepsilon(\lambda)/\mathcal{F}_0^{x_0/\varepsilon^2}\right] - \frac{2\varepsilon^2}{\pi}\mathrm{Re}\hat{C}_\eta^\varepsilon\right| \leq K_\delta e^{-C_\delta\lambda^2}\eta^2,$$
$$\hat{C}_\eta^\varepsilon = \sum_{i,j=1}^2\int_{x_0/\varepsilon^2}^{(x_0+\eta)/\varepsilon^2}\int_{x_1}^{(x_0+\eta)/\varepsilon^2}\mathbb{E}\left[\hat{c}_i(x_1,\lambda)\hat{c}_j^*(x_2,\lambda)V_i(x_1)V_j(x_2)/\mathcal{F}_0^{x_0/\varepsilon^2}\right]dx_2dx_1.$$

Now applying Lemma 10.4, we get $\left|\hat{C}_\eta^\varepsilon - \tilde{C}_\eta^\varepsilon\right| \leq K_\delta e^{-C_\delta\lambda^2}$, where

$$\tilde{C}_\eta^\varepsilon = \sum_{i,j=1}^2\int_{x_0/\varepsilon^2}^{(x_0+\eta)/\varepsilon^2}\int_{x_1}^{(x_0+\eta)/\varepsilon^2}\tilde{c}_i\tilde{c}_j^*(x,\lambda)\mathbb{E}\left[V_i(x_1)V_j(x_2)\right]dx_2dx_1.$$

By the stationarity of the processes V_j, the difference $\pi\eta g(x_0/\varepsilon^2,\lambda) - 2\varepsilon^2\mathrm{Re}\tilde{C}_\eta^\varepsilon$ goes to 0 as $\varepsilon \to 0$. Summing these inequalities establishes the result. □

We can now prove Proposition 6.1. Summing the inequalities of Lemmas 10.2 and 10.3 establishes that

$$\limsup_{\varepsilon\to 0}\left|\mathbb{E}\left[\bar{n}_\eta^\varepsilon(\lambda) - (x_\eta^\varepsilon - x_0)g(x_0/\varepsilon^2,\lambda)/\mathcal{F}_0^{x_0/\varepsilon^2}\right]\right| \leq K_\delta\eta^2 e^{-C_\delta\lambda^2} + K_\delta^\varepsilon(\lambda), \tag{40}$$

where the remainder

$$K_\delta^\varepsilon(\lambda) = \left|\mathbb{E}\left[(x_0+\eta-x_\eta^\varepsilon)\left(g(x_0/\varepsilon^2,\lambda) - g(x_\eta^\varepsilon/\varepsilon^2,\lambda)\right)/\mathcal{F}_0^{x_0/\varepsilon^2}\right]\right|$$

can be bounded by

$$K_\delta^\varepsilon(\lambda) \le \eta \sup_{(\nu,\mu)\in D_\delta, |\nu'-\nu|\le \eta^{\frac{1}{2}}, |\mu'-\mu|\le\eta^{\frac{1}{2}}} \left| g(\nu',\mu',\lambda) - g(\nu,\mu,\lambda)\right|.$$

Since the autocorrelation functions of the processes V_j are bounded by $\|V_j\|_\infty^2 \phi$ which satisfies $t \mapsto t\phi(t) \in L^1$, their Fourier transforms $d_j(k)$ have uniformly bounded derivatives. A short study of the function $(\nu,\mu)\mapsto g(\nu,\mu,\lambda) := -4G_1(\nu,\mu,\lambda)$ then shows that it is of class $\mathcal{C}^1$, and that there exists constants K_δ and $C_\delta > 0$ such that the derivatives of g are uniformly bounded with respect to $(\nu,\mu)\in D_\delta$ by $K_\delta e^{-C_\delta \lambda^2}$. This yields $K_\delta^\varepsilon(\lambda) \le K_\delta \eta^{3/2} e^{-C_\delta\lambda^2}$, and substituting into (40) we get

$$\limsup_{\varepsilon\to 0} \left| \mathbb{E}\left[\bar{n}_\eta^\varepsilon(\lambda) - (x_\eta^\varepsilon - x_0) g(x_0/\varepsilon^2, \lambda)/\mathcal{F}_0^{x_0/\varepsilon^2}\right] \mathbb{I}_{x_0 \le X_\delta^\varepsilon} \right| \le K_\delta \eta^{3/2} e^{-C_\delta\lambda^2}. \tag{41}$$

From Lemma 10.1 we have $\left|\bar{n}_\eta^\varepsilon(\lambda) - n(x_0^\varepsilon, x_\eta^\varepsilon,\lambda)\right| \le K_\delta |\bar{n}_\eta^\varepsilon(\lambda)|^2$. Under the adiabatic approximation, it can be checked from (18) that we have $\bar{n}_\eta^\varepsilon(\lambda) \le K_\delta \eta e^{-C_\delta\lambda^2}$. As a consequence we can substitute $n(x_0^\varepsilon, x_\eta^\varepsilon,\lambda)$ for $\bar{n}_\eta^\varepsilon(\lambda)$ in the left-hand side of (41). Application of Lemma 10.1 then completes the proof of Proposition 6.1. □

10.4. Mixing lemmas. In this subsection V is assumed to be a bounded, stationary, and zero-mean process satisfying a ϕ-mixing condition, with $\phi \in L^{1/2}(\mathbb{R}^+)$. Throughout the paper we use Lemma IV-4 of [16] that we state here.

LEMMA 10.4. *For any $\mathcal{F}_t^\infty$-measurable function $h(t)$ bounded by 1 satisfying $\mathbb{E}[h(t)] = 0$ for every t, we have, for any $t \le \tau \le u$,*

$$\left|\mathbb{E}\left[h(\tau)h(u)/\mathcal{F}_0^t\right] - \mathbb{E}\left[h(\tau)h(u)\right]\right| \le 4\phi(u-\tau)^{\frac{1}{2}}\phi(\tau - t)^{\frac{1}{2}}.$$

The following result is then a corollary of this lemma.

LEMMA 10.5. *The following limit is uniform with respect to k:*

$$\lim_{\varepsilon\to 0} \varepsilon^2 \mathbb{E}\left[\left| \int_{L/\varepsilon^2}^{(L+\delta L)/\varepsilon^2} V(t) e^{ikt} dt \right|^2 / \mathcal{F}_0^{L/\varepsilon^2} \right] = d(k)\delta L,$$

where $d(k) = 2\int_0^\infty \mathbb{E}[V(0)V(t)]\cos(kt)dt$.

Proof. Writing the square modulus of the integral as a double integral and applying Lemma 10.4 readily yields the result. □

REFERENCES

[1] M. J. ABLOWITZ AND H. SEGUR, *Solitons and the Inverse Scattering Transform*, SIAM, Philadelphia, PA, 1981.

[2] L. ARNOLD, G. PAPANICOLAOU, AND V. WIHSTUTZ, *Asymptotic analysis of the Lyapunov exponent and rotation number of the random oscillator and applications*, SIAM J. Appl. Math., 46 (1986), pp. 427–450.

[3] R. CARMONA AND J. LACROIX, *Spectral Theory of Random Schrödinger Operators*, Birkhauser, Boston, 1990.

[4] P. DESVILLARD AND B. SOUILLARD, *Polynomially decaying transmission for the nonlinear Schrödinger equation in a random medium*, J. Statist. Phys., 43 (1986), pp. 423–439.

[5] B. DOUCOT AND R. RAMMAL, *Invariant imbedding approach to localization*, J. Phys, 48 (1987), pp. 527–546.

[6] J. GARNIER, *Theoretical and numerical study of solitons in random media*, internal report available online at http://www.cmap.polytechnique.fr/users/www.garnier/garnier.html.

[7] I. S. Gradshteyn and I. M. Ryzhik, *Table of Integrals, Series, and Products*, Academic Press, San Diego, 1980.

[8] A. Hasegawa and F. Tappert, *Transmission of stationary nonlinear optical pulses in dispersive dielectric fibers,* I: *Anomalous dispersion*, Appl. Phys. Lett., 23 (1973), pp. 142–144.

[9] H. A. Haus and W. S. Wong, *Solitons in optical communications*, Rev. Mod. Phys., 68 (1996), pp. 423–444.

[10] V. A. Hopkins, J. Keat, G. D. Meegan, T. Zhang, and J. D. Maynard, *Observation of the predicted behavior of nonlinear pulse propagation in disordered media*, Phys. Rev. Lett., 76 (1996), pp. 1102–1105.

[11] V. I. Karpman, *Soliton evolution in the presence of perturbations*, Phys. Scripta, 20 (1979), pp. 462–478.

[12] Y. S. Kivshar, S. A. Gredeskul, A. Sanchez, and L. Vasquez, *Localization decay induced by strong nonlinearity in disordered systems*, Phys. Rev. Lett., 64 (1990), pp. 1693–1696.

[13] R. Knapp, *Transmission of solitons through random media*, Phys. D, 85 (1995), pp. 496–508.

[14] R. Knapp, G. Papanicolaou, and B. White, *Nonlinearity and localization in one dimensional random media*, in Disorder and Nonlinearity, F. K. Abdullaev, D. K. Campbell, and S. Pnevmaticos, eds., Springer-Verlag, Berlin, 1989, pp. 2–26.

[15] W. Kohler and G. Papanicolaou, *Power statistics for wave propagation in one dimension and comparison with transport theory*, J. Math. Phys., 14 (1973), pp. 1733–1745; 15 (1974), pp. 2186–2197.

[16] H. J. Kushner, *Approximation and Weak Convergence Methods for Random Processes*, MIT Press, Cambridge, 1984.

[17] S. V. Manakov, S. Novikov, J. P. Pitaevskii, and V. E. Zakharov, *Theory of Solitons*, Consultants Bureau, New York, 1984.

[18] A. C. Newell and J. V. Moloney, *Nonlinear Optics*, Advanced Topics in the Interdisciplinary Mathematical Science, Addison-Wesley, Redwood City, CA, 1992.

[19] G. Papanicolaou, D. Stroock, and S. R. S. Varadhan, *Martingale approach to some limit theorems*, in Statistical Mechanics and Dynamical Systems, D. Ruelle, ed., Duke Turbulence Conf., Duke Univ. Math. Series III, Part VI, Duke University, Durham, NC, 1976, pp. 1–120.

[20] W. Rudin, *Real and Complex Analysis*, McGraw–Hill, New York, 1974.

[21] H. Yoshida, *Construction of higher order symplectic integrators*, Phys. Lett. A, 150 (1990), pp. 262–268.